University of Reading

A transport hiatus in the North Atlantic Current in early 2014 led to the coincident trans-Atlantic heat and salt anomaly dipoles of 2015

Article

Published Version

Creative Commons: Attribution 4.0 (CC-BY)

Open Access

Allan, D. and Allan, R. P. ORCID: https://orcid.org/0000-0003-0264-9447 (2026) A transport hiatus in the North Atlantic Current in early 2014 led to the coincident trans-Atlantic heat and salt anomaly dipoles of 2015. Atmosphere-Ocean, 64 (2). pp. 159-180. ISSN 1480-9214 doi: 10.1080/07055900.2025.2590699 Available at https://centaur.reading.ac.uk/127108/

It is advisable to refer to the publisher's version if you intend to cite from the work. See Guidance on citing.

To link to this article DOI: http://dx.doi.org/10.1080/07055900.2025.2590699

Publisher: Taylor & Francis

All outputs in CentAUR are protected by Intellectual Property Rights law, including copyright law. Copyright and IPR is retained by the creators or other copyright holders. Terms and conditions for use of this material are defined in the End User Agreement.

University of Reading

www.reading.ac.uk/centaur

CentAUR

Central Archive at the University of Reading

Reading's research outputs online

Atmosphere-Ocean

ISSN: 0705-5900 (Print) 1480-9214 (Online) Journal homepage: www.tandfonline.com/journals/tato20

A Transport Hiatus in the North Atlantic Current in Early 2014 Led to the Coincident Trans-Atlantic Heat and Salt Anomaly Dipoles of 2015

David Allan & Richard P. Allan

To cite this article: David Allan & Richard P. Allan (2026) A Transport Hiatus in the North Atlantic Current in Early 2014 Led to the Coincident Trans-Atlantic Heat and Salt Anomaly Dipoles of 2015, Atmosphere-Ocean, 64:2, 159-180, DOI: 10.1080/07055900.2025.2590699

To link to this article: https://doi.org/10.1080/07055900.2025.2590699

© 2025 The Author(s). Published by Informa UK Limited, trading as Taylor & Francis Group

Published online: 15 Dec 2025.

Submit your article to this journal

Article views: 578

View related articles

View Crossmark data

Full Terms & Conditions of access and use can be found at
https://www.tandfonline.com/action/journalInformation?journalCode=tato20

Check for updates

A Transport Hiatus in the North Atlantic Current in Early 2014 Led to the Coincident Trans-Atlantic Heat and Salt Anomaly Dipoles of 2015

David Allan [1] and Richard P. Allan [2,*]

[1]*The Dell, St Albans, UK*
[2]*Department of Meteorology and National Centre for Earth Observation, University of Reading, Reading, UK*

[Original manuscript received 24 April 2025; accepted 11 November 2025]

ABSTRACT *Speculation surrounds the possibility that increasing world temperatures could trigger a decrease in the heat supplied to the Subpolar North Atlantic (SPNA) by the Gulf Stream (GS) and its extension, the North Atlantic Current (NAC). Here we provide evidence for just such a drop in heat and salt delivery in 2014, leading to the development of a cold fresh anomaly (CFA) in the SPNA and reciprocal warm salty anomaly (WSA) near North America in 2015. These coincident dipoles of heat and salt anomalies first appeared in February–March 2014 when cooling and freshening in the NAC near 45°N, 42°W was reciprocated by warming and increased salinity near 42°N, 50°W. The negative anomalies subsequently migrated north-eastwards along the path of the NAC to constitute the CFA centered on 50°N, 30°W by July 2015 while the reciprocal positive anomalies spread south-westwards to constitute the WSA centered on 40°N, 70°W. Sea surface temperature and height anomaly data revealed a rectangular three-fold structure for the CFA representing the path of the cooled and freshened NAC across the Mid-Atlantic Ridge. Surface current velocity data for early 2014 showed that northwards transport in the NAC was temporarily reversed near its exit from the Mann Eddy, possibly due to an influx of Labrador Sea Water from the Deep Western Boundary Current. We conclude that the unprecedented cooling/freshening of the SPNA and warming/salinification of the North American coastal region in 2014–2015 were reciprocal consequences of an interruption of northwards mass transport in the NAC near its exit from the Mann Eddy.*

RÉSUMÉ *[Traduit par la rédaction] Des spéculations entourent la possibilité que la hausse des températures mondiales puisse entraîner une diminution de la chaleur fournie à l'Atlantique Nord subpolaire (ANSP) par le Gulf Stream (GS) et son extension, le courant de l'Atlantique Nord (CAN). Nous fournissons ici des preuves d'une telle baisse de l'apport de chaleur et de sel en 2014, qui a mené au développement d'une anomalie froide et fraîche (AFF) dans l'ANSP et d'une anomalie chaude et salée (ACS) réciproque près de l'Amérique du Nord en 2015. Ces dipôles coïncidents d'anomalies thermiques et salines sont apparus pour la première fois en février-mars 2014, lorsque le refroidissement et l'adoucissement observés dans le CAN près de 45 N, 42°O ont été compensés par un réchauffement et une hausse de la salinité près de 42°N, 50°O. Les anomalies négatives ont ensuite migré vers le nord-est le long de la trajectoire du CAN pour former l'AFF centrée sur 50°N, 30°O en juillet 2015, tandis que les anomalies positives réciproques se sont propagées vers le sud-ouest pour former l'ACS centrée sur 40°N, 70°O. Les données relatives à la température et à l'anomalie de hauteur de la surface de la mer ont révélé une structure rectangulaire à trois volets pour l'AFF, représentant la trajectoire du CAN refroidi et rafraîchi à travers la dorsale médio-atlantique. Les données sur la vitesse des courants de surface pour le début de 2014 ont montré que le transport vers le nord dans le CAN s'est temporairement inversé près de sa sortie du tourbillon de Mann, peut-être en raison d'un afflux d'eau de la mer du Labrador provenant du courant profond de la frontière occidentale. Nous concluons que le refroidissement/rafraîchissement sans précédent de l'ANSP et le réchauffement/salinisation de la région côtière nord-américaine en 2014–2015 ont été les conséquences réciproques d'une interruption du transport de masse vers le nord dans le CAN près de sa sortie du tourbillon de Mann.*

KEYWORDS North Atlantic Current; Labrador Current; Deep Western Boundary Current; Heat/Salt Anomaly Dipole; Mann Eddy

*Corresponding author's email: r.p.allan@reading.ac.uk; Lead author email: dna.allan@btinternet.com

© 2025 The Author(s). Published by Informa UK Limited, trading as Taylor & Francis Group. This is an Open Access article distributed under the terms of the Creative Commons Attribution License (http://creativecommons.org/licenses/by/4.0/), which permits unrestricted use, distribution, and reproduction in any medium, provided the original work is properly cited. The terms on which this article has been published allow the posting of the Accepted Manuscript in a repository by the author(s) or with their consent.

1 Introduction

a *The Significance of Heat and Salt Anomalies in the North Atlantic*

There has been great recent interest in the possibility that an observed cooling and freshening of the central region of the North Atlantic could be associated with a decrease in transport of heat and salt from the sub-tropics to northern latitudes via the Gulf Stream (GS)/North Atlantic Current (NAC) which forms part of the Atlantic Meridional Overturning Circulation (AMOC). Such a change would of course have important consequences for North Atlantic climate in general. Much of the work in this area has considered the long-term pre-2014 cold anomaly (so-called 'warming hole' or Cold Blob) originally described by Dima and Lohmann (2010) and Drijfhout et al. (2012) and subsequently investigated by others interested in possible links to recent changes in AMOC (Rahmstorf et al., 2015; Robson et al., 2016; Caesar et al., 2018, 2021; Gervais et al., 2018; Keil et al., 2020; Boers, 2021; Li et al., 2022; Allan & Allan, 2019, 2024; Rahmstorf, 2024). As we have noted previously (Allan & Allan, 2024, 2025), this long-term cold anomaly was largely the product of major cooling events associated with periods of ice release from the Arctic and sub-Arctic Odden region between 1970 and 1995 which seem unlikely to have had any connection with AMOC strength now.

Some attention has turned to the unusual short-term cooling and freshening of the subpolar North Atlantic (SPNA) between 2014 and 2016 (Bryden et al., 2020; Desbruyères et al., 2019; Frajka-Williams et al., 2017; Grist et al., 2016; Holliday et al., 2020; Josey et al., 2018; Sanders et al., 2022; Stendardo et al., 2020) which contrasted sharply with rising temperatures in the rest of the global ocean during this period (Yin et al., 2018). In this work we refer specifically to the 2014–2016 feature as the cold fresh anomaly (CFA) and as pointed out by Josey et al. (2018), Holliday et al. (2020) and Sanders et al. (2022), it is important to distinguish this short-term CFA from the long-term so-called 'warming hole'.

Grist et al. (2016) attributed the acute cooling of the eastern SPNA (our CFA) to unusually strong air–sea fluxes caused by exceptionally low air temperatures in early 2014 but this would not have explained the concomitant drop in salt concentration in this region which Holliday et al. (2020) described as the "the largest freshening event for 120 years in the eastern subpolar North Atlantic" and of considerably larger magnitude than the three 'Great Salinity Anomalies' of the late 20th century (Belkin et al., 1998) which were associated with Arctic ice release, ice and iceberg accumulation on the Flemish Cap and the appearance of the 'warming hole' (Allan & Allan, 2024, 2025).

Holliday et al. (2020) suggested that a wind-driven rerouting of Arctic-derived fresh water in the Labrador Current (LC), perhaps channelled from the Newfoundland Basin via the NAC, caused the acute freshening of the eastern SPNA observed in 2014–16. They also noted that this freshening in the SPNA appeared to be balanced by increased salinity in the western North Atlantic near the coast of North America, forming a trans-Atlantic dipole of salinity anomalies. A similar salinity dipole, but also coinciding with an ocean heat content (OHC) dipole, was noted by Frajka-Williams et al. (2017) and Bryden et al. (2020). Stendardo et al. (2020) also remarked that negative/positive salinity anomalies in the SPNA/subtropics appeared to mirror the distribution of SST anomalies. The 2014 freshening identified by Stendardo et al. (2020) was in the region associated with the reticulations of the North Atlantic Current (NAC) as it crosses the Mid-Atlantic Ridge (MAR) and this extends the hypothesis that the 2014–16 event involved a freshening and (presumably) cooling of the path of the NAC east of 40^{o}W. The work presented here supports that idea but rather than the Labrador Current being the source of cooling we suggest that the heat and salt dipoles were the result of a brief hiatus in mass transport in the NAC beginning in early 2014. This would be expected to have had measurable consequences for North Atlantic climate.

b *The Oceanographic Background*

Heat and salt transport from the subtropics to the SPNA are thought to occur largely via the GS and its extension, the NAC (Fig. 1a) but few specific changes in the transmission of heat and salt by these currents have been identified which might illuminate the mechanism of cooling and freshening in the SPNA in 2014–2016. Dong et al. (2019) did find a slight weakening and southward movement of the GS at 38^{o}N together with a decrease of sea surface height (SSH) in 2014 but others have found little evidence for a marked change in flow in the GS at 38^{o}N between 1993 and 2013 (Liu et al., 2020; Palter, 2015). A small reduction in meridional heat transport at 26°N was apparent from 2009–2012 but anomalies between 2014 and 2016 were unremarkable (Bryden et al., 2020; Liu et al., 2020). Although Gonçalves Neto et al. (2021) interpreted increases in sea surface height and SST at 50^{o}W as evidence for a sustained northerly shift of the GS from 2008, the authors of a long-term study of the GS path (Seidov et al., 2019) remarked that the stability of the GS between 75^{o}W and 50^{o}W (1965–2017) was "nothing less than spectacular".

This GS stability changes remarkably near 40^{o}N 46^{o}W, the corner of the Newfoundland Ridge which extends south-eastwards from the Tail of the Grand Banks (TGB) (Fig. 1b). Here Klein and Siedler (1989) demonstrated a bifurcation of GS flow to form the North Atlantic Current (NAC) proceeding generally north-eastwards towards the SPNA and the Azores Current (AC) directed initially south-westwards before continuing eastwards along the latitude line 33^{o}-34^{o}N, south of the Azores (Fig. 1a). The work of Krauss et al. (1990) confirmed this branching of the GS (accounting for 80 Sv of current flow) into the NAC (50 Sv) and AC (30 Sv) near 41^{o}N 45^{o}W. A more recent analysis of surface currents in this region (Caldeira & Reis, 2017) identifies the GS branch point close to 40^{o}N 46^{o}W (Fig. 1b). The proximity

2026 La Société canadienne de météorologie et d'océanographie

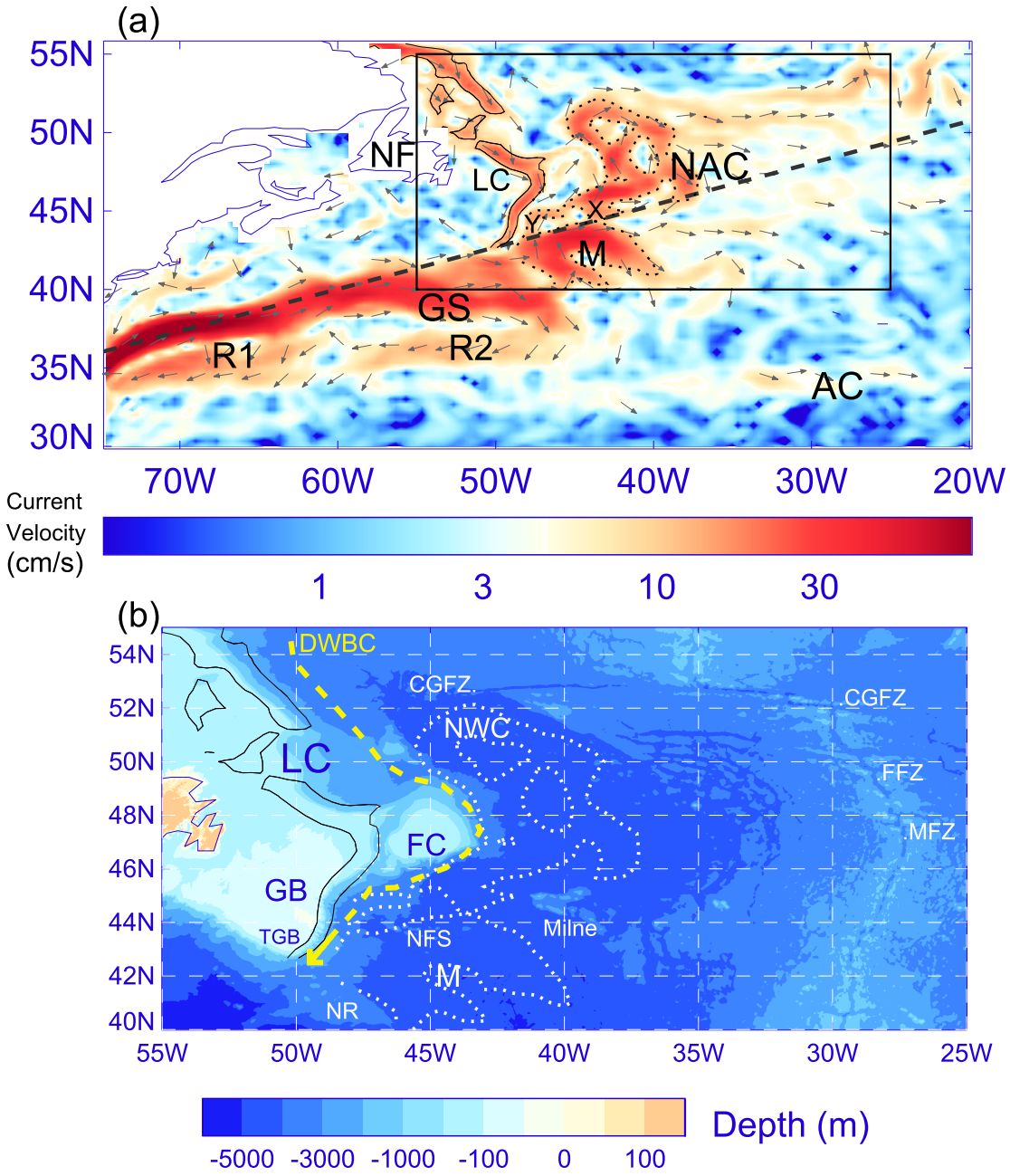

Fig. 1 **(a) Surface current velocity near Newfoundland (mean 1993–2013).** Sea surface currents were characterised in terms of velocity and direction according to the protocol of Caldeira and Reis (2020) using the OSCAR data from NOAA. Arrows indicate direction for currents with velocity >6cm/s. GS is Gulf Stream, AC is Azores Current, LC is Labrador Current; NAC is North Atlantic Current. NF marks Newfoundland, R1, R2 mark two major recycling pathways along the path of the GS. A transect line (dashed) between 36°N 75°W and 50°N 19°W is utilized in Figures 5,6. A streamline defined by mean surface current of 13 m/s constitutes an approximate climatological mask encompassing the strongest currents in this region. Outline paths of the NAC (dotted line) and LC (solid line) are indicated and replicated in Figure 1b; the NAC outline is employed in Figures 1b, 8 and 9. The color bar indicates current velocity in cm/s log scale. **b) Relation of the NAC and LC to bathymetry in the Newfoundland Basin.** Area shown is the rectangle in Figure 1a. Outline mask of the NAC (dotted line) is derived from Figure 1a. DWBC is indicated by a yellow dashed line. CGFZ, FFZ and MFZ mark Charlie-Gibbs, Faraday and Maxwell fracture zones (CGFZ, 52.5°N 43°-30°W, FFZ, 49.5°N 27.5°W and MFZ, 47°N 27°W respectively). Also marked are the Grand Banks (GB), Flemish Cap (FC), Tail of the Grand Banks (TGB), Newfoundland Seamounts (NFS), Milne Seamounts (Milne) and Northwest Corner (NWC). X and Y mark major exits of the NAC from the Mann Eddy (M).

of this point to the Newfoundland Ridge suggests the possibility that this geomorphological feature could be an influential factor in the separation of the NAC and the AC because like the GS, the NAC generally occupies channels >3500m deep (Carr & Rossby, 2001; Rossby, 1996) whereas the Newfoundland Ridge presents a barrier which is <3000m deep over large areas. As previously demonstrated by Qiu (1994), Caldeira and Reis (2017) and Jacobs et al. (2020)

there is evidence for the existence of strong recirculation currents south and north of the GS between 75°W and 50°W (e.g. R1 and R2 in Fig. 1a). Later studies have found larger values for the NAC flow rate near 42°N than the 50Sv calculated by Krauss et al. (1990). These have ranged from about 64–146 Sv (see Pérez-Brunius et al., 2004) but the higher values most likely included the northward circulation of the Mann Eddy (M in Fig. 1a,b), a large semi-permanent anticyclonic gyre which forms part of the initial NAC circulation and borders on the GS bifurcation point (Mann, 1967; Rossby, 1996). A more recent flow estimate for the NAC east of the Flemish Cap at 47°N was about 110Sv (Mertens et al., 2014). An increase in the flow rate of the NAC compared with the GS would not be surprising considering the considerable momentum which could be added by the LC as it joins the GS/NAC near the TGB (Fratantoni & McCartney, 2010).

As shown in Fig. 1a which is based on the mean of surface current velocity data (1993–2013), the NAC is initially part of the rising limb of the Mann Eddy from which it exits to the north near 45°N 43°W (X in Fig. 1b) through the 200km gap between the most easterly of the Newfoundland Seamounts ('Shredder,' <3000m depth, 44°N 43.5°W, see Fig. 1a) and the most westerly of the Milne seamounts (45°N 41°W, about 2000m depth, see Fig. 1b). This appears to be the major route (Fig. 1a) but we will refer later to a less prominent route (Y) where the flow exits from the east of the Mann Eddy near 44°N 48°W (Fig. 1a). The NAC then passes east of the Flemish Cap and proceeds around Northwest Corner (NWC, Lazier, 1994; Rossby, 1996) before turning east where it subdivides into several main channels as it negotiates the complex geomorphology of the Mid-Atlantic ridge (MAR, Fig. 1b). A major return current is evident at about 38°-39°W which likely corresponds to the southward-flowing Newfoundland Basin Return Current identified by Bower and von Appen (2008), Mertens et al. (2014) and Stendardo et al. (2020) that may augment flow in the descending (eastern) limb of the Mann Eddy.

Bower and von Appen (2008) identified two major branches of the NAC crossing the MAR and showed that this branching may in part be defined by the major fracture zones in the MAR (Charlie-Gibbs, CGFZ at 52°-53°N and Faraday, FFZ at 49°-50°N; Fig. 1b). A rather similar pattern of two main branches was identified by Breckenfelder et al. (2017) from observations and models: a northern branch which was propagated via Northwest Corner at 52°N and partly impinging on the path of the CGFZ and a branch near 50°N which crossed the MAR close to the FFZ. Although their work did not fully cover the region of the CGFZ and did not examine the region east of 30°W, Stendardo et al. (2020) identified essentially the same two branches as noticed by the earlier workers but in addition they described a third (southern) branch in a region not covered by Bower and von Appen (2008) or by Breckenfelder et al. (2017) at latitudes 42°-46° where a considerable proportion of the flow crossing 45°W appeared to be recycled to the west and south. Daniault et al. (2016) also proposed a three-branched structure corresponding to the CGFZ, FFZ and the Maxwell fracture zone (MFZ) at 47°N 27°W (Fig. 1b).

Fig. 1a shows two major eastward channels across the MAR (mean of 2012–2020) corresponding approximately to the CGFZ and the FFZ (see caption for definitions) as described by Bower and von Appen (2008) for 1993–2005 and Breckenfelder et al. (2017) for 1993–2008. There is a third, more complex channel between 43°N and 46°N which may correspond to the MFZ and resembles the 'southern branch' of the NAC described by Stendardo et al. (2020). Thus, Fig. 1a suggests a three-fold path of the NAC across the MAR as concluded by Stendardo et al. (2020) although these authors noted that there was some additional eastward flow south of 45°N and this is evident in Fig. 1a. A similar conclusion was reached by Daniault et al. (2016). The pattern shown in Fig. 1a for 1993–2013 is therefore consistent with previous analyses of the path of the NAC across the MAR but extends to some areas not completely covered by past reports.

Fig. 1a,b also illustrates the path of the LC south of 55°N, the main branch of which passes along the eastern flank of the Grand Banks (GB) generally inshore of the 500m isobath, before retroflecting to meet the GS near the TGB (Allan & Allan, 2025; Fratantoni & McCartney, 2010; Han et al., 2008; Jutras et al., 2023; Solodoch et al., 2020a). It is important to remember that the path of the inshore LC south of 50°N is largely over water <500m deep whereas the paths of the GS and the NAC as far as 40°W are generally over water which is >4000m deep (Fig. 1b). This disparity becomes obvious east of the TGB where cold, fresh and dense LC water has the potential to descend more than 2000m into the GS/NAC (Krauss et al., 1990; Rossby, 1996).

We should emphasize that these **surface** current velocity observations may not tell us much about the major south-directed cold current in the Newfoundland Basin: the Deep Western Boundary Current (DWBC) which mainly passes east of the Flemish Cap (Mertens et al., 2014) before occupying the **deep** water in the narrow space between the LC and the NAC (Zantopp et al., 2017). Here it has considerable opportunities to interact at depth with the adjacent NAC before probably merging with the LC near the Tail of the Grand Banks (see Fig. 1b). In some cases, researchers in this area have not convincingly distinguished between the near-surface LC (about 7.5 Sv; Fratantoni & McCartney, 2010) and the deep DWBC (about 30 Sv; Mertens et al., 2014; Zantopp et al., 2017).

Despite these reservations regarding the use of surface current velocity measurements to follow the path of deep currents, in many cases these deep currents have surface manifestations which have been interpreted as proxies for the path of the main deep current. Examples of this protocol are provided by Caldeira and Reis (2017) who used surface current velocity data to follow the paths of the GS, NAC and Azores Current and Solodoch et al. (2020) who examined the paths of the DWBC and the NAC using the same technique. Thus, Fig. 1a is based on an accepted connection between surface current velocity/direction and deep current velocity/direction.

2026 La Société canadienne de météorologie et d'océanographie

c *The Rationale for this Work*

Here we present evidence for an interruption in the transport of warm salty water in the proximal NAC close to its exit from the Mann Eddy near 45°N 43°W (X) in February–March 2014. We reason that a short-term deficit in warm salty water delivered to the distal NAC would cause an influx of adjacent cold fresh Atlantic water into the path of the NAC. Onward delivery of this cooled and freshened NAC water along normal pathways would lead to the development of the CFA and we show that this is so because the CFA **is** the path of the NAC as it reticulates and slows while negotiating the complexities of the MAR.

If the CFA is the result of an interruption of transport in the GS or NAC, then a quantity of warm salty water equivalent to that withheld from the NAC is likely to be rerouted elsewhere in early 2014. This could explain the trans-Atlantic heat and salt dipole which has been described previously (Bryden et al., 2020; Frajka-Williams et al., 2017; Holliday et al., 2020, see above) where a negative pole of heat and/or salt anomaly in the SPNA is balanced by a positive pole near the North American coast. There is a report of a warming near the North American seaboard which has been explained in terms of a northward movement of the GS but this was in 2008 and not 2014–2016 (Gonçalves Neto et al., 2021). Evidence has also been presented for decreased temperatures (Desbruyères et al., 2019; Grist et al., 2016; Josey et al., 2018) and salinity (Holliday et al., 2020) at depth in the SPNA in 2014–2016. In these cases, the changes were largely ascribed to local atmospheric or oceanic drivers but little attempt was made to explain the parallel development of warming and increased salinity near the North American seaboard thousands of kilometres west of the SPNA. The present work provides evidence that the heat and salinity dipoles which appeared in 2014–2015 were the natural consequence of a short hiatus in mass transport in the proximal NAC in early 2014.

2 Data and methods

Salinity and OHC data (Fig. 2, Fig. 3, Fig. 4 and Fig. 5) were derived from the UK Met Office EN4 version 2.2 analysis (Good et al., 2013) including the modifications proposed by Gouretski and Reseghetti, (2010) and were obtained from https://www.metoffice.gov.uk/hadobs/en4/. High resolution SST anomaly data (Fig. 6a, Fig. 7) was from the 1/4° Optimum Interpolation Sea Surface Temperature (OISST) V2 High Resolution Dataset provided by the NOAA PSL, Boulder, Colorado, USA (https://psl.noaa.gov). Monthly mean surface heat flux data (net shortwave and longwave radiation, sensible and latent heat) and precipitation minus evaporation from the European Centre Medium-range Weather Forecasts 5th generation reanalysis was, extracted from Copernicus https://cds.climate.copernicus.eu/. Copernicus was also the source of data for the zonal (u) and meridional (v) components of absolute surface geostrophic current velocity (Fig. 8, Fig. 9). SSH (sea surface height) anomaly data was from Copernicus Gridded L4 Sea Surface Heights and Derived Variables Reprocessed 1993 to present, spatial resolution 0.125° × 0.125° based on the period 1 Jan 1993–8 Sep 2023.

Combined surface current velocity patterns (Fig. 1a) were derived from the Ocean Surface Current Analysis Real-time (OSCAR) sea surface velocity dataset estimated from sea surface height, surface vector wind and sea surface temperature based on multiple satellites and *in situ* instruments since 1992 and constrained by a physical fluid dynamics model (from https://podaac.jpl.nasa.gov). Version 1.4 data at a 1/3 degree latitude and longitude resolution is provided over the period 1993–2013. Zonal and meridional currents are averaged and marked as missing if more than 30% of the data is invalid, e.g. due to ice cover. Mean flow current velocity and direction is calculated from the mean zonal and meridional flows and displayed with a logarithmic scale (Fig. 1a).

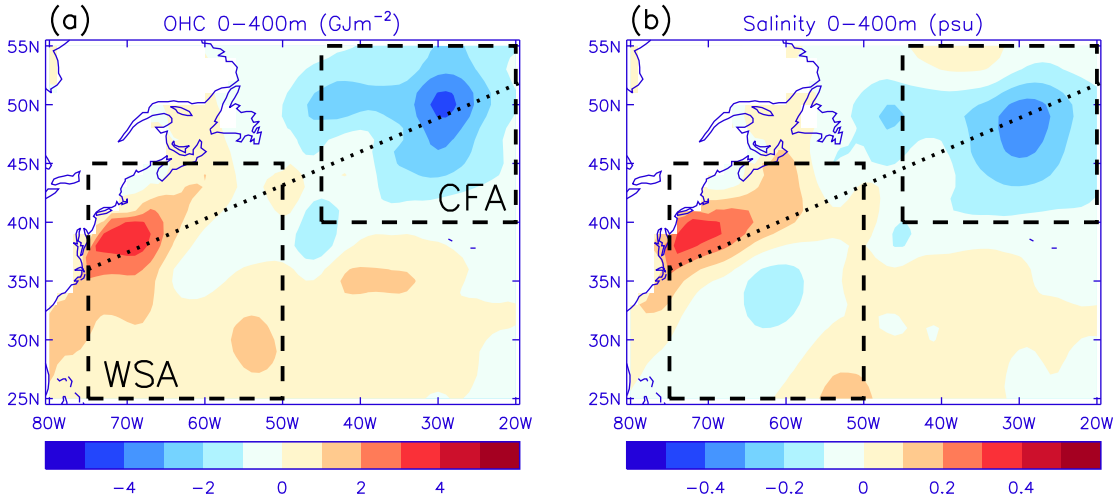

Fig. 2 Latitude-longitude plots of 0–400m anomalies of (a) Ocean heat content (OHC, GJ/m^2) and (b) salinity (psu) in the North Atlantic in July 2015 (EN4 2.1). The most intense areas of positive/negative anomaly are referred to in the text as WSA/CFA epicentre (40 °N 70 °W/ 50 °N 30 °W) respectively. Dashed rectangles outline the areas referred to later as the WSA region (25°–45°N, 75°–50°W) and the CFA region (40°–55°N 45°–20°W). The dotted line in Figure 2a,b is a transect between 36°N 75°W and 51°N 20°W defined in Figure 1. Anomalies are calculated relative to the 1990–2012 means.

2026 Canadian Meteorological and Oceanographic Society

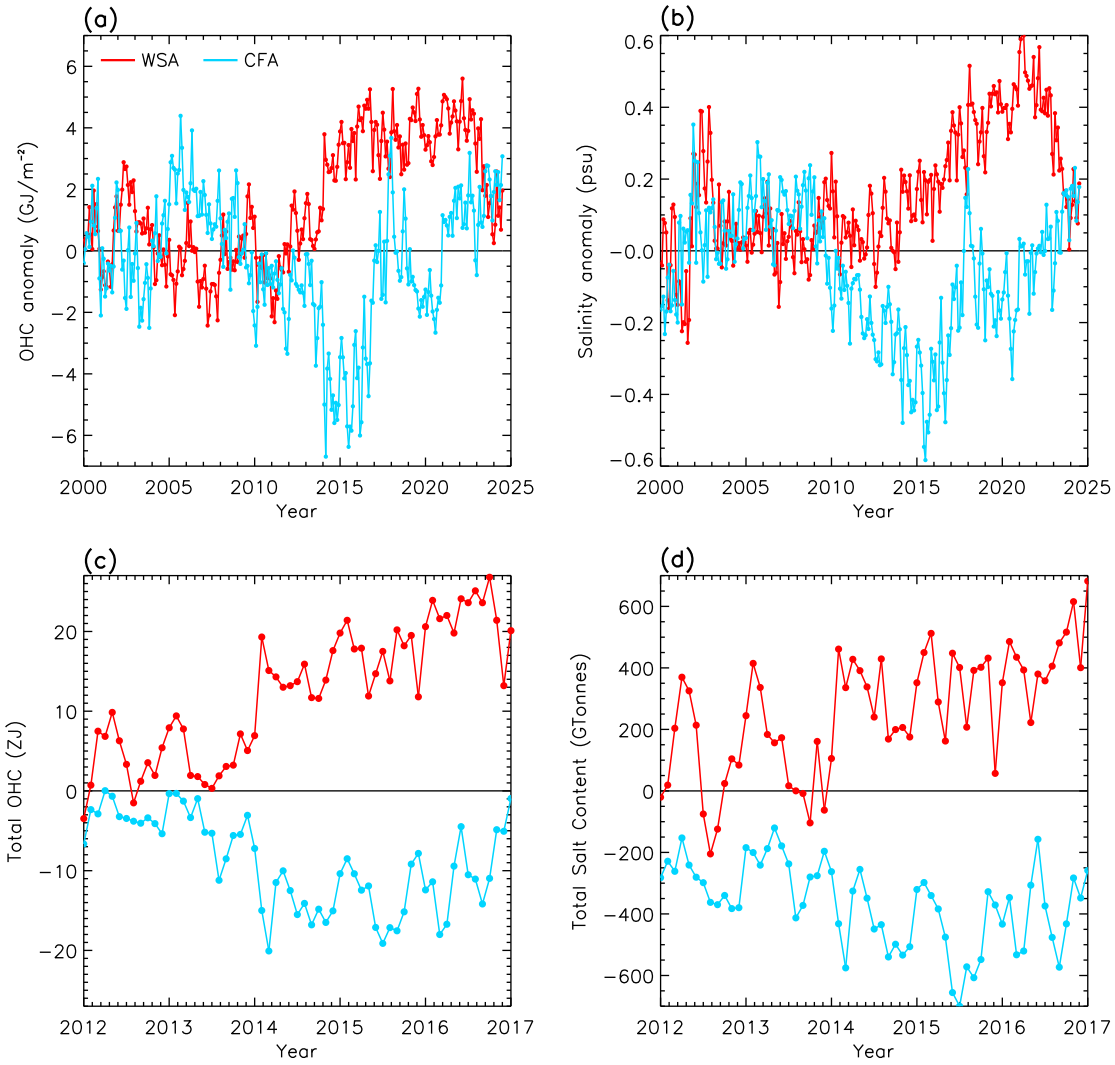

Fig. 3 Comparison of the time series of 0-400m anomalies of (a) OHC (GJ/m^2); (b) salinity (psu); (c) total OHC (ZJ) and (d) total salt content (GTonnes) for the WSA region (25°–45°N 75°–50°W) (red) and the CFA region (40°–55°N 45°–20° W) (blue) as illustrated in Figure 2a,b. Values for anomalies were monthly deseasonalised and relative to means for 2002-2012. Values for total heat (c) and salt (d) are derived by multiplying the time series of anomalies of OHC (J/m^2) and salinity (psu, practical salinity units) by the respective areas of the two sectors (5.1 and 2.9 million km^2 for WSA and CFA respectively) and for salinity, multiplying further by the depth (400m). Land area in the WSA region was excluded from the calculation of sea area. psu values were converted into salt content using the identity 1psu=1kg salt/m^3. One ZJ is 10^{21}Joules.

The latitude/longitude positions of selected oceanographic features were obtained from IHO-IOC GEBCO Gazetteer of Undersea Feature Names, at www.ngdc.noaa.gov/gazetteer. Distances and ocean depth were assessed using Google Earth Pro. Data acquisition and analysis has been greatly facilitated by the employment of KNMI Climate Explorer (https://climexp.knmi.nl/).

3 Results

a *Anomalies of Heat and Salt are Reciprocal Between the CFA and the WSA*

Fig. 2 compares the 0–400m anomalies of ocean heat content (OHC) and salinity in the North Atlantic in July 2015 when the CFA was strongest. It identifies the Cold Fresh Anomaly (CFA) as the region centred near 50°N 30°W which exhibits deep **negative** anomalies of OHC (a) and salinity (b) and the WSA (Warm Salty Anomaly) centred close to 39°N 70°W near the path of the GS (Caldeira & Reis, 2017; Rossby, 1996; Fig. 1a) which shows deep **positive** anomalies of heat and salinity. These findings are similar to those described by Bryden et al. (2020) and with respect to salinity, closely resemble those reported by Holliday et al. (2020) who noted the salty/fresh dipole characteristic of salt anomalies in the North Atlantic in 2014–2016. They are consistent with the temperature profile shown by Josey et al. (2018) which revealed a negative anomaly centered near 50°N 30°W from the surface to 500m depth and with the warming of the region near the North American continental shelf described by Gonçalves Neto et al. (2021). The transect

2026 La Société canadienne de météorologie et d'océanographie

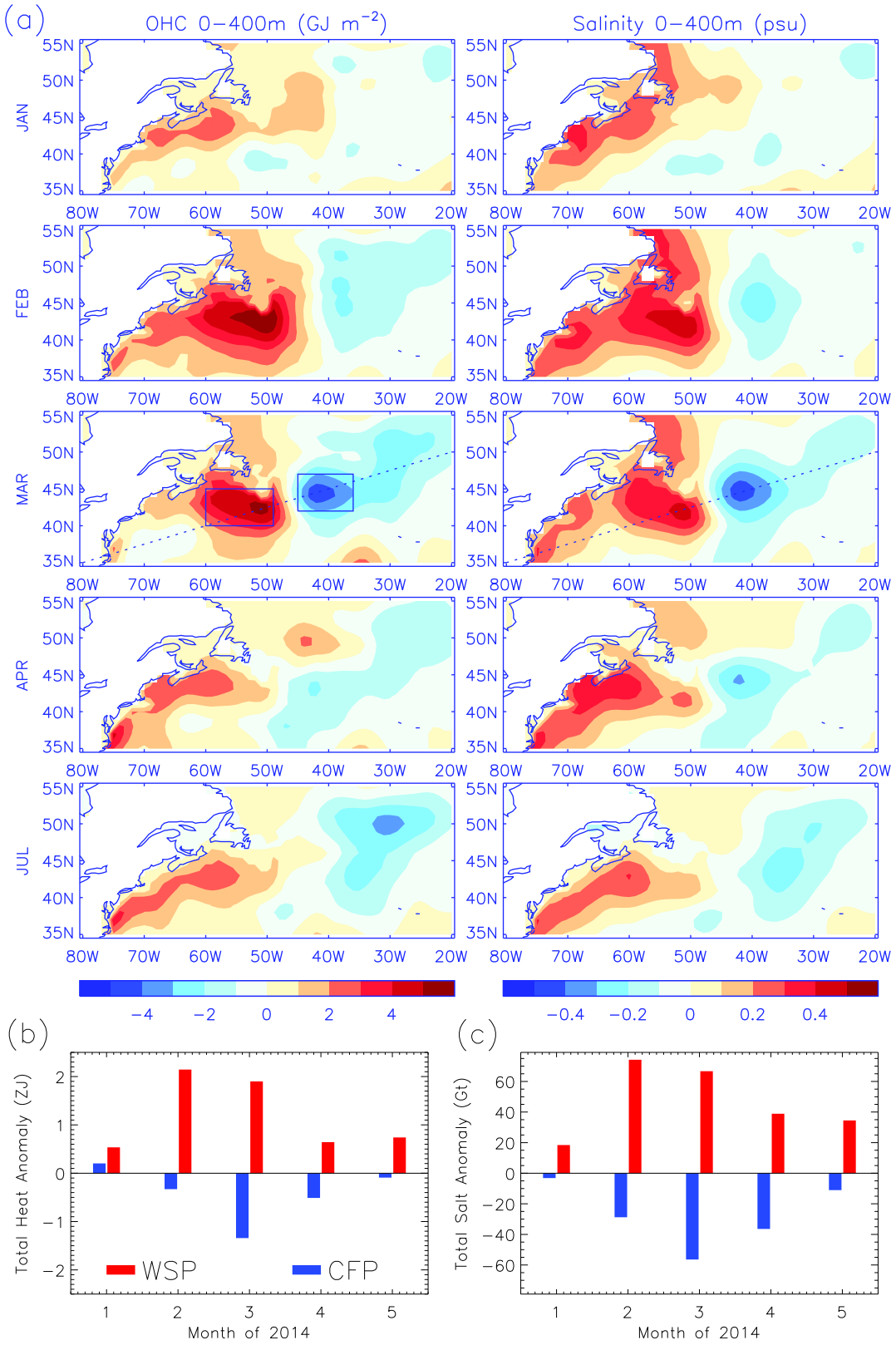

Fig. 4 (a) Latitude-longitude plots of 0–400m anomalies (relative to the 1990–2010 mean) of OHC and salinity between January and July 2014 for latitudes 35°–55°N and longitudes 80°-20°W. A transect line between 36°N, 75°W and 51°N, 19°W (black dotted line) in the March panels is utilized in Figure 5. The rectangular boxes displayed in the March 2014 OHC panel enclose the epicenters of the WSP (warm salty pole, 40°–45°N 60°–49°W, 4.9×10^{5}km^2) and CFP (cold fresh pole, 42°-47°N 45°-36°W, 4.2×10^{5}km^2). More quantitative estimates of the anomalies of (b) total OHC 0–400m (ZJ) and (c) salt content 0–400m (GTonnes) measured within the rectangular boxes displayed in Figure 1a are shown in the top 400m of ocean between January and May 2014 (labelled months 1–5).

2026 Canadian Meteorological and Oceanographic Society

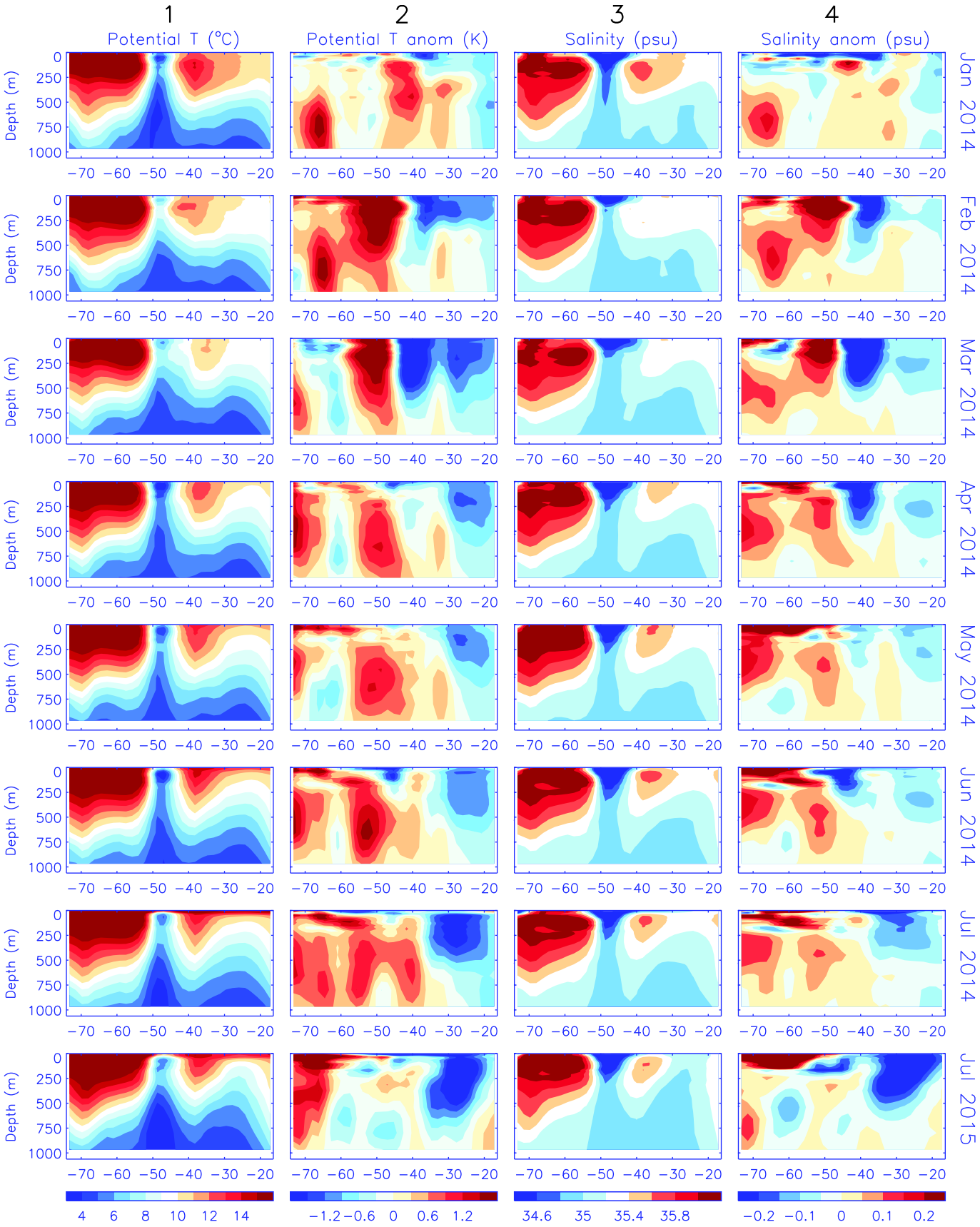

Fig. 5 Changes with depth (0–1000m) in potential temperature (°C, column 1), salinity (psu, column 3) and anomalies of these two parameters (columns 2 and 4 respectively) for selected months in 2014 and 2015 along a transect line from 36°N 75°W to 51°N 19°W shown in Figure 1a. Horizontal axis is longitude.

2026 La Société canadienne de météorologie et d'océanographie

line 36°N 75°W to 51°N 19°W was defined in Fig. 1 and chosen to pass close to the centers of the CFA and WSA so that we could investigate the evolution of the dipoles prior to July 2015. July 2015 was chosen for Fig. 2 because that represented the time of maximum development of the trans-Atlantic dipole of heat and salt which had been noticed by Bryden et al. (2020) and Holliday et al. (2020).

Fig. 3a,b represent the anomaly time series from 2000 to 2024 of ocean heat content (OHC) and salinity at 0–400m depth for the CFA and WSA regions defined by the two boxes marked with dashed lines in Fig. 2a,b. These areas were chosen to encompass most of the main regions of change in the CFA and WSA between 2014 and 2015, particularly allowing for the observation (not pursued here) that some heat and salt migrated south and east of the main WSA region near the N. American coast in 2014. It is evident that in the period 2014–2016 there was a substantial reduction in heat (Fig. 2a) and salt (Fig. 2b) content in the CFA and corresponding increases of comparable magnitude in the WSA. After 2015 there was a gradual return to long term mean values for the CFA but heat and salt remained elevated in the WSA. The 2014–2017 event was by far the largest change in the whole period since 2000 and we concentrate on this period in Fig. 3c,d which compare changes in total OHC and salt content in the top 400m of the WSA and CFA marked by dashed lines in Fig. 2. These total values were derived by multiplying the values seen in Fig. 3a,b by the respective areas of the CFA and WSA (Fig. 2).

The changes in total heat content in the CFA (Fig. 3a) seen in 2014–16 consisted of a series of downturns in early 2014, late 2014, mid-2015 and 2016 which were interspersed with a series of upturns of which the most prominent was in early 2015 when the anomaly temporarily returned to the normal range. Only in the initial downturn of about 8ZJ in the CFA in January to February 2014 was there a clear corresponding upturn of about 8ZJ in heat anomaly in the WSA, opening the possibility that heat was diverted from the CFA into the WSA. The magnitude of this initial reciprocal change of 8ZJ in the CFA/WSA in two months (5.2×10^6seconds) was equivalent to a change in power of about 3×10^{15} J/s or 3PW which is more than the reported total power of the GS (about 1.3PW at 38°N, Palter et al. 2015; Liu et al., 2020). Bubnov (1995) found a value of 2PW for the power of the NAC and Pérez-Brunius et al., (2000) measured a power of 3.5PW for the NAC near its origin (42°N) and including the rising limb of the Mann Eddy, Fig. 1) so our result for the drop in power of the NAC of about 3PW is equivalent to a large decrease of total NAC flow in early 2014.

A similar approximate reciprocity between the CFA and WSA regions was seen for the time series of salinity anomalies (Fig. 3b) and the magnitude of the freshening/salinification respectively in early 2014 was equivalent to the removal/addition of about 400 Gtonnes (400 $x10^{12}$ kg) of salt from/to the CFA/WSA. The mean volume of fresh water to be added to this amount of salt to reach the reference salinity of 35 psu ($35kg/m^3$) is about 10,000 km^3 (for 0–400m) which is a similar order of magnitude to the estimate of 6600 km^3 reported by Holliday et al. (2020) for the fresh water equivalent of the 2014–16 salt deficit (0–1000m) which these authors described as "the largest freshening event for 120 years in the eastern SPNA". The changes in OHC in 2014–16 were similarly much larger than any seen before or after (Fig. 3a).

There was a highly significant correlation between OHC and salinity time series values January 2014-June 2016 in the CFA (r = 0.89) and WSA (r = 0.87; Fig. 3c,d). For the 30 months of this period the ratio of salt (10^9 tonnes, Gtonnes) to OHC (10^{21} Joules, ZJ) anomalies was 34 ± 5 (± 1 standard deviation) for the CFA and 23 ± 12 for the WSA and contrasted with the wildly variable ratios for the whole period 1995–2024 for the CFA (11 ± 292) and WSA (55 ± 269). The high correlation between OHC and salinity anomalies in the 2014–2016 period implied that heat and salt anomalies in both the CFA and WSA were linked and largely changed in unison. The initial rapid changes in heat and salt anomaly in early 2014 were dramatic but there were indications of further intensification of the negative anomalies in the CFA region in late 2014, mid-2015 and early 2016 (Fig. 3c,d). Thus, whatever the cause of the initial reduction of heat and salt in the CFA in 2014, it appears to have been repeated subsequently, alternating with periods of recovery.

b *The Early Evolution of the CFA and WSA*

Fig. 2 is a snapshot in July 2015 which reveals positive and negative anomalies of heat (a) and salt (b) corresponding respectively to the WSA near the North American continental shelf and the CFA in the SPNA. This disposition of heat and salt anomalies resembles the salt anomaly 'dipole' described by Holliday et al., (2021) and we will use this terminology to include both salt and OHC anomalies. To determine how the 2015 dipoles (Fig. 2a,b) developed we investigated the initial changes in heat and salt in early 2014. Latitude-longitude plots were constructed for salinity and OHC at 0–400m depth covering the changes seen in Fig. 3 in the months January to July 2014 (Fig. 4). The results confirm the development in February and March 2014 of dipoles comprising the warm/salty pole (WSP) which was most intense in February in the western sector south of the Grand Banks and the cold/fresh pole (CFP) in the eastern SPNA and most intense in March. These dipoles appeared to be the precursors of the WSA and CFA of Fig. 2 but far closer together, in a much smaller area and close to 40°W compared with the WSA at 70°W and the CFA at 30°W more than a year later (Fig. 2). By July 2014 the dipoles had separated into approximately the positions of the WSA and CFA seen a year later (Fig. 2). The months March to July 2014 in Fig. 4a show the progressive drift of cold anomalies eastward towards the CFA epicentre near 50°N 30°W and warm anomalies westward towards the North American coast. Thus, the WSP and CFP may have been the initial dipoles of salt and OHC anomalies in February–March 2014 which preceded the

2026 Canadian Meteorological and Oceanographic Society

subsequent development of the WSA and CFA (Fig. 2). We leave open the possibility that they could be intrinsically different.

The month of maximum intensity of the WSP (February) preceded that of the CFP (March) as seen also in Fig. 3. Quantitative changes were assessed in the sectors defined by 40°-45°N 60°-49°W (0.49 million km^2) and 41°-47°N 45°-36°W (0.42 million km^2) (rectangles in Fig 4a, March OHC panel) which are only about 10% and 16% respectively of the large WSA and CFA areas compared in Fig. 3. The total anomalies of heat (Fig. 4b) and salt (Fig. 4c) content between January and April confirm the observation in Fig. 4a that the increase of both parameters in the WSP was maximal in February while the maximum for the CFP was in March. Broadly the values for maximal heat and salt anomalies in the WSP in March 2014 are reciprocal to those in the CFP although we have not accounted for the drift of intensity eastwards from the CFP which is particularly visible in March (Fig. 4a). At present we have no explanation for the disjunction between the time series of changes in the WSP compared with those in the CFP but it may be useful to re-examine the events in 2014 at greater depths than 400m.

From Fig. 4b, the ratio of total salt to heat is 35GT/ZJ for the WSP and 42GT/ZJ for the CFP, similar to the values for the WSA and CFA (see above). The values for total salt and heat content anomalies for the WSP and CFP in March 2014 (about 2ZJ and 60GT respectively) are about a quarter of the anomalies observed in July 2015 for the whole WSA and CFA regions (Fig. 3, about -8ZJ and -250GT) over an area which is about ten times greater than the WSP and CFP (see above). Thus, about a quarter of the heat and salt anomalies seen in the CFA and WSA in July 2015 were already identified by March 2014 in the CFP and WSP within much smaller areas. The precise value is likely to be greater because from Fig. 3a, substantial positive heat and salt anomalies had already moved westwards towards North America by February and negative anomalies had moved northeastwards towards the CFA by March so were not included in the above calculation based on the areas within the rectangles illustrated. Thus, we have underestimated the CFP.

This is a dynamic situation and the OHC and salinity parameters which are essential for characterizing the mass changes involved are of relatively low resolution both in space (1°) and time (1 month) compared with the focus and rapidity of events. Accurate quantification is made difficult by these factors.

Although these are relatively crude estimates of the heat and salt changes involved, the results present a coherent picture which shows that a considerable proportion of the total heat and salt changes in 2014–15 occurred in the early months of 2014 within adjacent areas (WSP and CFP) near Newfoundland which are only about 10% of the eventual areas of the WSA and CFA (Fig. 2). The scale of these changes is very large and comparable with the normal capacity of the NAC to transport heat and salt into the SPNA. It was also fast, occurring within a month or two although full restoration to normal conditions took about two years.

The position of the CFP in Fig. 4 is significant because it appears to represent the point where the coldness and freshness of the CFA first emerges before it subsequently moves northeast to concentrate near 50°N 30°W. This initial location is centered on 44.5°N 42.5°W and corresponds approximately to the path of the NAC where it emerges from the northern section of the Mann Eddy (X in Fig. 1b is centered on 44.5°N 43.5°W). Thus, the CFP lies in the narrow (200km) channel of NAC water deeper than 4000m approximately between the Newfoundland Seamount chain, the Milne Seamounts (<2500m depth, 45°N 41°W) (Fig. 1a,b) and the margin of the Flemish Cap where NAC flow is likely to be most constricted. It is surprising that such large negative anomalies of heat and salt should accumulate here in early 2014 and that equivalent positive anomalies should accumulate near the TGB at 41°N 51°W. The progressive separation of the warm/salty and cold/fresh poles between February and July 2014 and ultimately July 2015 (Fig. 2) is an important feature, the possible mechanism of which we will discuss later (Discussion).

c *Subsurface Changes in Heat and Salt During the Evolution of the CFA and WSA*

Fig. 5 follows changes in salinity and temperature for 0–1000m depth along a transect line (Figs. 1,2,4) between 36°N 75°W and 51°N 19°W which passes through the epicenters of the WSA and CFA in July 2015 (Fig. 2) and the WSP and CFP in March 2014 (Fig. 4). It covers the period from January 2014 (when changes were first seen) to July 2015 when CFA anomalies were greatest (Fig. 3). This transect line drawn on the map of North Atlantic currents (Fig. 1a) also passes through the northern section of the GS between 70°W and 60°W, close to the TGB, through the LC near 42°N 49°W and through the NAC north of the Mann Eddy near 44°N 42°W.

The major features were identified on the depth-time series (Fig. 5) in terms of potential temperature (column 1) and salinity (column 3) and were seen in all such plots between 2010 and 2019 (not shown). The first of these was a wedge of very warm (>15°C) and very salty (> 36 psu) water between 75°W and 50°W extending from the surface to about 300m depth; this represents the GS as seen in terms of current velocity in Fig. 1a. The raw salinity data (column 3) shows indications of segregation between the 70°W and 60°W intersections of the transect line with the GS (Fig. 1a).

The second feature was a very cold (<5°C) fresh (< 34.8 psu) narrow column of water at about 43°N 49°W extending from close to the surface down to at least 1000m. The topmost section of this column could correspond to the region where the LC passes southwards along the shallow continental shelf of the Grand Banks to meet the GS (Krauss et al., 1990; Rossby, 1996; Fratantoni & McCartney, 2010; Fig.

2026 La Société canadienne de météorologie et d'océanographie

1a). The main component which occupied the column from 250m to 1000m is most likely to represent the Labrador Sea Water (LSW) the upper major constituent of the Deep Western Boundary Current (DWBC) which occupies the narrow strip of deep water between the LC and the NAC (Fig. 1b; see Zantopp et al., 2017). Indeed, there was some indication of a separation between a near surface component in the top few hundred meters and a deep component which extended down at least as far as 1000m.

The third feature was a warm (about 14°C) salty (about 35.7 psu) layer extending from the surface to about 500m depth between 43°W and 37°W which would include the point where the main channel of the NAC exits the Mann Eddy near 45°N 43°W (X in Fig. 1) but could include other parts of the NAC extending further east. Later, we refer to the above three features as GS, LC/DWBC and NAC regions respectively.

Beginning in February 2014 there were dramatic changes in the distribution of temperature and salinity (columns 1 and 3 respectively) and their anomalies (columns 2 and 4 respectively). The temperature in the top 400m of the LC/DWBC region (column 1) rose from about 5°C (January) to 8°C (February) and salinity rose from about 34.5 to 34.9psu (column 3) while the NAC region dropped from about 14°C to about 11°C and from 35.7 psu to 35.2 psu. These changes were reflected in the temperature and salt anomalies (columns 2 and 4 respectively) for February and March which were strongly positive (about +3°C and 0.4psu) near 50°W but strongly negative (-3°C and -0.4psu) near 42°W corresponding to the region of the NAC north of the Mann Eddy which had been identified previously (Fig. 1,4). During February and March these adjacent anomalies formed a positive/negative dipole although the development of the positive anomaly slightly preceded that of the negative anomaly both for heat and salt as in Fig. 4. By June 2014 the LC/DWBC and NAC regions had largely been restored to their original state in January 2014 (columns 1 and 3) and the considerable anomalies of temperature and salinity at 50°W and 40°W had faded away.

To assess the contribution of surface heat exchanges to the heat content changes, monthly heat fluxes were computed from the European Centre for Medium range Weather Forecast 5th generation reanalysis (Hersbach et al., 2020) for the CFP and WSP boxes as a sum of net downward shortwave and longwave surface radiative fluxes plus sensible and latent heat fluxes. The maximum anomalous heating of +69 Wm^{-2} (relative to 1990–2010) in the WSP region occurred in January 2014 and was determined by reduced sensible and latent heat flux loss, while greater absorbed shortwave radiation was balanced by increased longwave radiative heat loss. This net heat input equates to 0.18 GJm^{-2} which is an order of magnitude smaller than the observations-based estimated increases in upper ocean heat content of about 3 GJm^{-2} (Fig. 4). Similarly, the strongest anomalous cooling of the CFP of -54 Wm^{-2} in February 2014 equates to 0.14 GJm^{-2}, small compared to the upper 400m heat content change of about -2.4 GJm^{-2} from February to March 2014. Surface fresh water fluxes computed from precipitation minus evaporation anomalies are as large as +2.1 mm/day in January 2014 for the CFP and -2.0 mm/day in March 2014 over the WSP. While contributing to surface salinity anomalies, these cannot explain the large upper 400m ocean salinity changes. Consequently, it is very difficult to explain how air–sea exchanges alone could explain a large drop in salinity in the CFP or parallel rises in heat and salinity in the WSP.

Together with these changes in intensity of the anomalies of heat and salt, there were indications that the positive anomalies progressively moved westwards towards the North American continental shelf and the negative anomalies moved eastwards from about 40°W in March to near 30°W in July 2014 and within the CFA region (see Fig. 1). These movements were observed as early as February for the near surface negative temperature anomaly (column 2) but progressed rapidly eastwards through March and April so that by August 2014 most of this negative anomaly was seen centered on the CFA epicentre near 50°N 30°W. An increase in heat and salt positive anomalies near the North American coast close to the WSA epicentre (70°-75°W) was seen as early as March and was concentrated near the surface. By July 2014 the westward progress of these positive anomalies was not complete although it was by July 2015 (see also Fig. 1b). These findings are consistent with the results shown in Fig. 4 and reinforce the idea that the CFA is the manifestation of anomalously cooler, fresher NAC water moving into the manifold of the MAR and replacing warmer saltier water which normally would be delivered to this region. The large anomalies of heat and salt seen in February -March 2014 correspond to the WSP and CFP in Fig. 4 which it can be seen extend to depths greater than 500m.

d *The Evolution of the CFA as Defined by OISST and SSH Anomalies in 2013–2014*

From Fig. 4 and 5 there is a strong inference that the development of the CFA involves a cooling of the path of the NAC which begins just north of the Mann Eddy and spreads out across the reticulations of the MAR. This cannot be confirmed with the 1° resolution afforded by OHC and salinity data so we used anomalies of OISST (Optimum Interpolation Sea Surface Temperature) and SSH (Sea Surface Height) data (both parameters having 0.25° resolution) to follow the development of the CFA in 2013–2014 (Fig. 6). By definition, OISST represents surface temperature whereas SSH is sensitive to thermal expansion/contraction of the water column (Kelly et al., 1998) and therefore to changes in temperature at depth (but not at the surface) although the two parameters yield comparable results for the initial changes in 2014.

In December 2013 OISST anomalies were largely positive but between January and May 2014 there was a progressive intensification of negative anomalies in a roughly rectangular region between 40°-55°N and 40°-20°W (Fig. 6a)

2026 Canadian Meteorological and Oceanographic Society

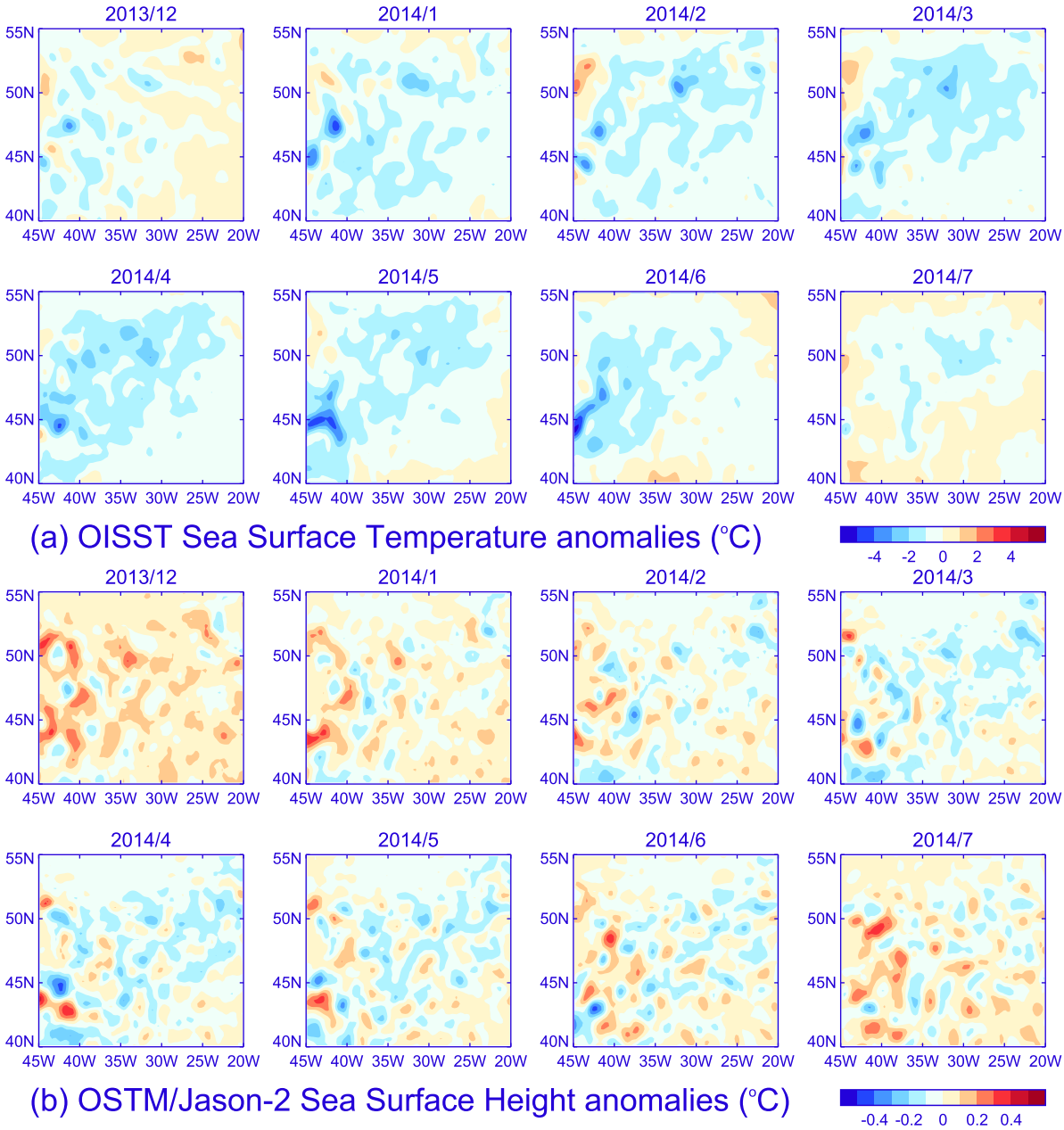

Fig. 6 The fine structure of the CFA in 2013-2014 as visualised by (a) OISST anomalies (°C) relative to a 1996–2012 baseline and (b) sea surface height (SSH) anomalies (m) relative to 1993–2012. Latitude-longitude plots of monthly anomalies of (a) OISST and (b) SSH between 40°N-55°N and 45°W and 20°W are compared between December 2013 and July 2014.

corresponding to the CFA (Fig. 3) which showed indications of a threefold east–west branching particularly in March 2014. Cold anomalies diminished by June 2014 and had largely disappeared by July. A similar pattern of negative (cold) anomalies was seen using SSH to probe changes in the CFA region between December 2013 and July 2014 (Fig. 6b). In December 2013 the SPNA was largely occupied by positive (warm) SSH anomalies but by January 2014 more negative anomalies appeared and these increased through February to April when anomalies were almost entirely negative, corresponding to the rectangular region of negative OISST anomalies in Fig. 6a. From May, positive anomalies progressively reappeared until by July anomalies were predominantly positive again. The pattern of negative anomalies was consistent in suggesting a division into three east–west sections (at approximately 50°-53°N, 45°-50°N and 43°-47°N) between March and May and similar to the threefold division of the OISST anomalies seen in Fig. 6a. In February to May with both OISST and SSH there was a prominent spot at about 50°N 31°W but neither this nor any of the other spots of greater negative anomaly could be obviously related to any apparent bathymetric feature. However, there was a well-

2026 La Société canadienne de météorologie et d'océanographie

defined spot at 45°N 43°W between March and May in Fig. 6b and a similar but less well-defined spot in Fig. 6a which coincided with the position of the CFP (Fig. 4a) and X in Fig. 1b.

The maximum mean ocean temperature anomaly in the CFP (48°-52°N 32°-28°W) was about -1.5 °C in early 2014 in the top 400m (Josey et al. (2018) and assuming a mean water temperature of about 8°C at 500m depth and hence a value of about 1.5×10^{-4} / °C for the thermal expansion coefficient (TEC) of seawater (Roquet et al., 2022) then the expected change in SSH simply due to thermal expansion of the water column would be about -0.1 m. This is consistent with the observed mean SSH anomaly value in the CFA in April of about -0.1 m (Fig. 6a). SSH is also influenced by halosteric factors in the North Atlantic (Pardaens et al., 2011; Stendardo et al., 2016, 2020); assuming an approximate haline contraction coefficient of 7.8×10^{-4} $(g/kg)^{-1}$ (Roquet et al., 2022) the observed -0.2 psu anomaly in early 2014 (Fig. 5) corresponds with a contraction of the upper 400m slightly smaller and of opposite sign to the temperature effect (+0.06 m). We assume subsequently that SSH anomaly variations are more strongly related to thermal expansion or contraction of a deep column of seawater as originally suggested by Kelly et al. (1998). Other factors such as wind patterns and interaction of currents with bottom topography also affect SSH, but these are expected to be small variations in monthly anomaly data and on a wider scale than the 0.25° resolution of SSH.

e *The CFA is a Manifestation of the Branching of the NAC as it Crosses the MAR*

Previously the CFA has been perceived as an amorphous 'blob' largely because the parameters employed to quantify it (HadSST, OHC, salinity) only resolved to 1° of latitude and longitude. The higher resolution of SSH and OISST anomalies (both 0.25°) allowed a comparison of the structure of the CFA with other probes of NAC structure based on current velocities which also have high resolution (Bower & von Appen, 2008; Breckenfelder et al., 2017 and Stendardo et al., 2020). Fig. 7a shows the structure of the CFA in March 2014 as revealed by the largely negative OISST anomalies. The overall shape is quasi-rectangular with three main zonal sections which correspond approximately to the positions of the three major fracture zones CGFZ, FFZ and MFZ (a). It has been suggested previously that the path of the NAC across the MAR might be influenced by the major fracture zones although there is considerable temporal variation in the precise path (Bower & von Appen, 2008). There were periods when the CFA region was occupied by largely positive anomalies (e.g. January 2013, Fig. 7c) but a similar rectangular structure is still evident. This suggests that the essential structure is independent of whether the anomaly is positive or negative and most likely is related to the underlying geomorphology.

This idea is supported by Fig. 7b,d which shows a survey of the same region using SSH anomalies (b,d) instead of OISST anomalies (a,c). Again, in March 2014, there is a rectangular approximately three-fold structure in (b) similar to that seen in (a) but extending further east to as far as 15°W and a similar pattern was also seen in Jan 2013 when anomalies were largely positive (d). As noted above, SSH is likely to be sensitive to changes in temperature deep in the ocean since unlike OISST it will respond to changes in thermal expansion (Kelly et al., 1998). The patterns (c) and (d) are quite similar, suggesting that these very different parameters are both sensitive to temperature and that surface changes follow much the same pattern as deeper changes, consistent with previous indications (Fig. 4,5) that the temperature changes in the CFA are not just superficial but extend below 500m. It should be noted that SSH generally gave slightly more stable and higher resolution patterns than OISST, a parameter necessarily subject to atmospheric influences which would hardly affect SSH because that is largely sensitive to mean temperature in the deep ocean and scarcely affected by the surface conditions (Kelly et al., 1998). The differences between the results for OISST (Fig. 7a) and SSH (Fig. 7b) were small, suggesting that ambient atmospheric variations were minor influences.

Fig. 7e,f shows the patterns of zonal (e) and meridional (f) surface current velocities in the same area in March 2014, giving a picture of the NAC structure (Fig. 1a) which can be compared with the patterns of OISST and SSH anomalies in Fig. 7a,b. The zonal surface velocity distributions (e) mark out approximately three major currents and correspond best with the SSH anomaly pattern (b) although the OISST distribution (a) is similar as far as 22°W. Meridional currents (f) can approximately be identified with meridional distributions of OISST (a) but more so with SSH (b) anomalies near 40°W, 30°W and 20°W.

OISST and especially SSH anomalies may thus provide a useful indicator not only for the path of the NAC in the CFA region where it crosses the MAR but from also from its origin as the CFP near 45°N 43°W where it separates from the Mann Eddy. This illuminates the finding from Fig. 4,5 that there was a movement of cold fresh anomalies along the path of the NAC which eventually slowed as it reached the complex manifold of the MAR. Thus, the CFA represented the path of the NAC as it branched and slowed while negotiating the reticulations of the MAR. That interpretation is consistent with the findings of Bower and von Appen (2008) that the zonal velocity of the NAC at the centre of the MAR close to the line of the CGFZ averaged about 5cm/s, much lower than the reported values of about 50cm/s east of Flemish Cap at about 40°W and depth 0–500m (Mertens et al., 2014). It can be seen that the general segregation of negative anomalies of SSH and SST (Fig. 7a,c) resembles that shown by Bower and von Appen (2008) for the branching of the NAC revealed by current velocity data. Our results are also consistent with the proposal of these authors that branching could be influenced by the position of the major fracture zones (CGFZ at 52°-53°N, FFZ at 49–50°N and MFZ at 47°N) (see also Dainault et al., 2016).

2026 Canadian Meteorological and Oceanographic Society

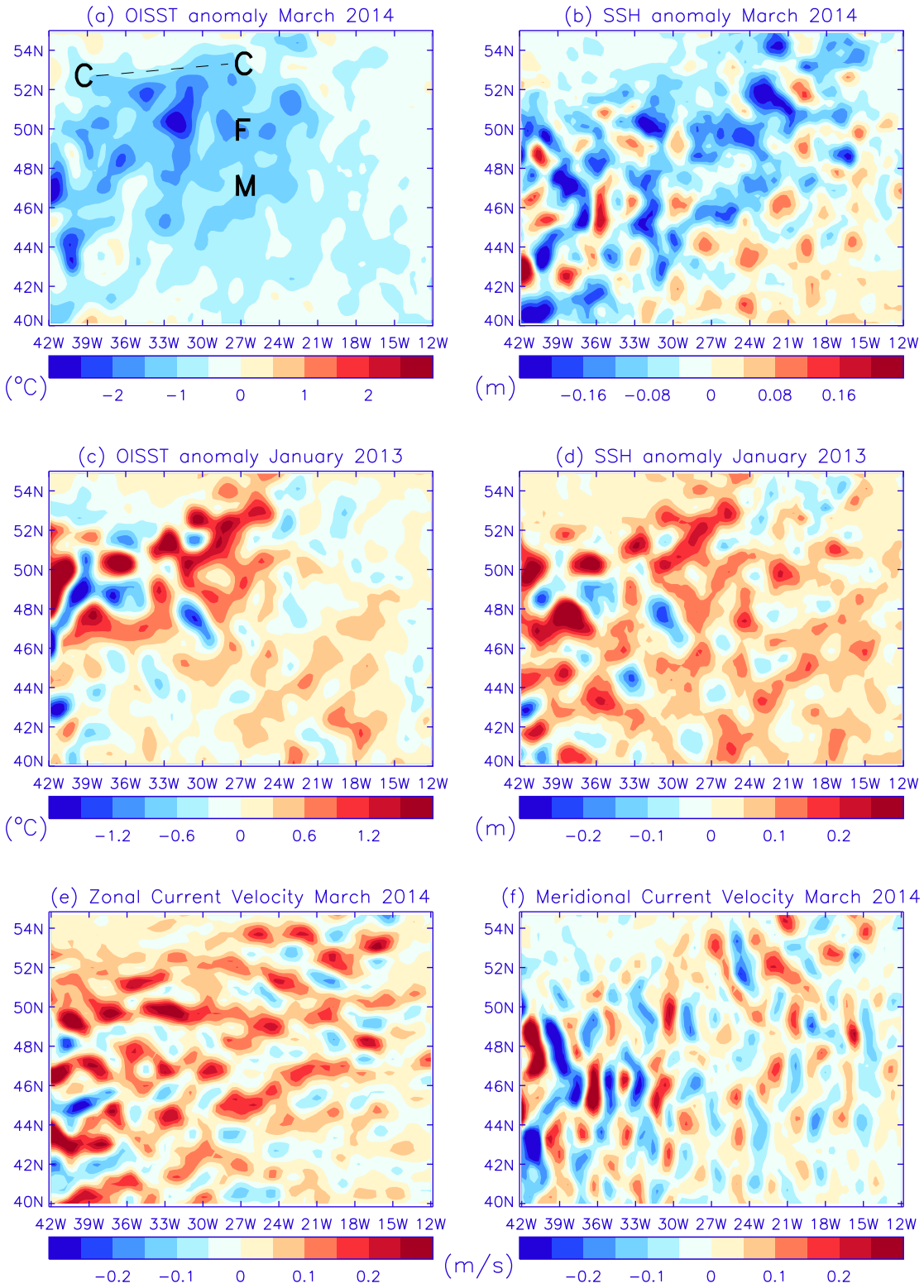

Fig. 7 The fine structure of the CFA region rendered as OISST (a,c) and SSH (b,d) anomalies in a cold month (March 2014, a,b) or a warm month (January 2013, c,d) compared with the path of the NAC across the MAR in March 2014 as assessed by zonal (e) or meridional (f) surface current velocity data. The approximate positions of the Charlie-Gibbs (C), Faraday (F) and Maxwell (M) fracture zones (see Figure 1b) are added to panel (a). Note that differing color scales are applied in a-d to emphasise key features.

2026 La Société canadienne de météorologie et d'océanographie

f *Changes in Ocean Surface Current Velocity in the Newfoundland Basin in 2014*

Finally, we sought some indication of changes in ocean surface currents in 2014 which could be associated with a possible hiatus in transport in the NAC. We chose as a baseline the meridional and zonal mean current velocities from 2008 to 2013 (the first panels in each of the two datasets a and b in Fig. 8) and there were few differences from these patterns seen in any previous 5y period or since 2016 (not shown). The mask of the path of the NAC inserted into these diagrams is based on the distribution of high current velocities shown in Fig. 1a,b so of course, the separated meridional and zonal components follow the same path generally northwards with the zonal currents filling in the horizontal gaps in the meridional pattern. Thus, the anticyclonic circulation of the Mann Eddy (M) is well-illustrated by the combination of northward/eastward (red) and southward/westward (blue) currents in the meridional and zonal patterns respectively. An important feature of these diagrams of the 5y mean values is that it implies that there are two possible exits to the north from the Mann Eddy, the most prominent one at about 44.5N 43.5°W in water around 4800m deep (X) and the other at about 45°N 48°W (Y) 3500m deep where there was an apparent gap (slower flow, referred to later as the Y gap) in the NAC mask. There was a subsequent common circulation past the Flemish Cap (Mertens et al., 2014), around Northwest Corner and either crossing the MAR or recirculating via the Newfoundland Basin Return Current (N).

The southward path of the LC is clearly shown in the meridional diagram (8a), skirting the edge of the Grand Banks as far as the TGB and in relatively shallow water (<500m, Fig. 1b). It needs to be remembered that surface current velocity measurements may not directly indicate the path of the DWBC which occupies the deep water between the LC and the NAC (>2000m, Fig. 1b).

We looked for any alterations in the meridional (8a) and zonal (8b) surface currents associated with the NAC in the period between January and May 2014 when large changes were seen in heat and salt content at 0–400m depth in the Newfoundland Basin (Fig. 5,6). On 31 January 2014 the main meridional currents (Fig. 8a) resembled in relative magnitude and position the respective 2008–2013 mean values and we noted the normal strong northwards (red) flow through the central exit from the Mann Eddy (X). However, there were indications of southward currents (blue) over the western Mann Eddy which may have had their origin either in the LC, the DWBC or the Newfoundland Basin Return current (R). There was also an apparent eastward displacement of the rising limb of the Mann Eddy which appeared to be associated with an eastward incursion of the LC/DWBC that was seen throughout the meridional time series between January and May. By Feb 15 a strong southerly flow (blue) had developed apparently from the direction of the LC/DWBC through the Y gap and during March this southerly flow became established at X, completely displacing the original northerly (red) flow and presenting as a most unusual reversal in the normal northward flow in the NAC. During the second half of April these changes gradually reversed and by May 17 a strong northward current became established again at X, restoring the continuity of the northward flow in the NAC. Throughout this period however, there was an apparent strong increase in the southward flow of what could have been the combined LC/DWBC at 42°N, 50°W close to the TGB.

The zonal data (Fig. 8b) for the same time period illustrated the northeastward-directed and westward-directed limbs of the Mann Eddy circulation and a possible confirmation of the easterly displacement of the rising limb in March and April (see above). This displacement appeared to be associated with a westerly-directed flow (blue) which became established in February–March in the exit region just to the north of the Mann Eddy (X) instead of the normal neutral zonal flow. This westerly-directed flow did not apparently stem from the LC/DWBC but was associated with enhanced currents from the east particularly in March. During this period of westerly-directed flow at X, there was an apparent southerly deflection of the normal easterly (red) flow of the Mann Eddy which appeared to extend east of the usual path of the NAC (March to April panels). By May 17 the normal easterly-directed flow at X and the continuity of the NAC were restored.

We consider that our evidence from meridional (8a) and zonal data (8b) indicates a reversal in current direction near the narrow exit (X) from the Mann Eddy near 44.5°N, 43.5°W which would represent a hiatus in the normal flow of the NAC northwards in Feb-Apr 2014. This implied that the lesion in NAC transmission was near the exit of the NAC from the Mann Eddy at 44.5°N, 43.5°W, which is close to the centre of the CFP in March (44.5°N, 42°W, Fig. 5,6). Thus, although the current reversal in early 2014 was nominally at the surface, it was coincident with large changes in heat and salt content at 0–400m depth especially in February–March 2014 (Fig. 4, Fig. 5).

It has been accepted that the LC normally contributes cold fresh water to the GS and NAC (Fratantoni & McCartney, 2010; Rossby, 1996), and there is evidence in Fig. 8a,b for an increased contribution of LC/DWBC water in early 2014 which might have promoted the current reversal at X and the formation of the CFP. Such an influx of LC water could correspond to the flow of 'Arctic' water posited by Holliday et al. (2020) to explain the salt dipole in 2014. However, the zonal data (Fig. 8b) suggests that increased current from the east reaching X predominates and this water is likely to be colder and fresher than the NAC. Thus, the influx of LC/DWBC water from the **west** could account for the current reversal at X which stops northward transport in the NAC and the apparent deflection of the path of the NAC seen in April 2014 (Fig. 8c). However, the major cooling and freshening of the NAC in 2014 could have been due to an influx of cold fresh water from the **east** (Fig. 8c) to replace the warm salty water which was no longer progressing along the path of the NAC.

2026 Canadian Meteorological and Oceanographic Society

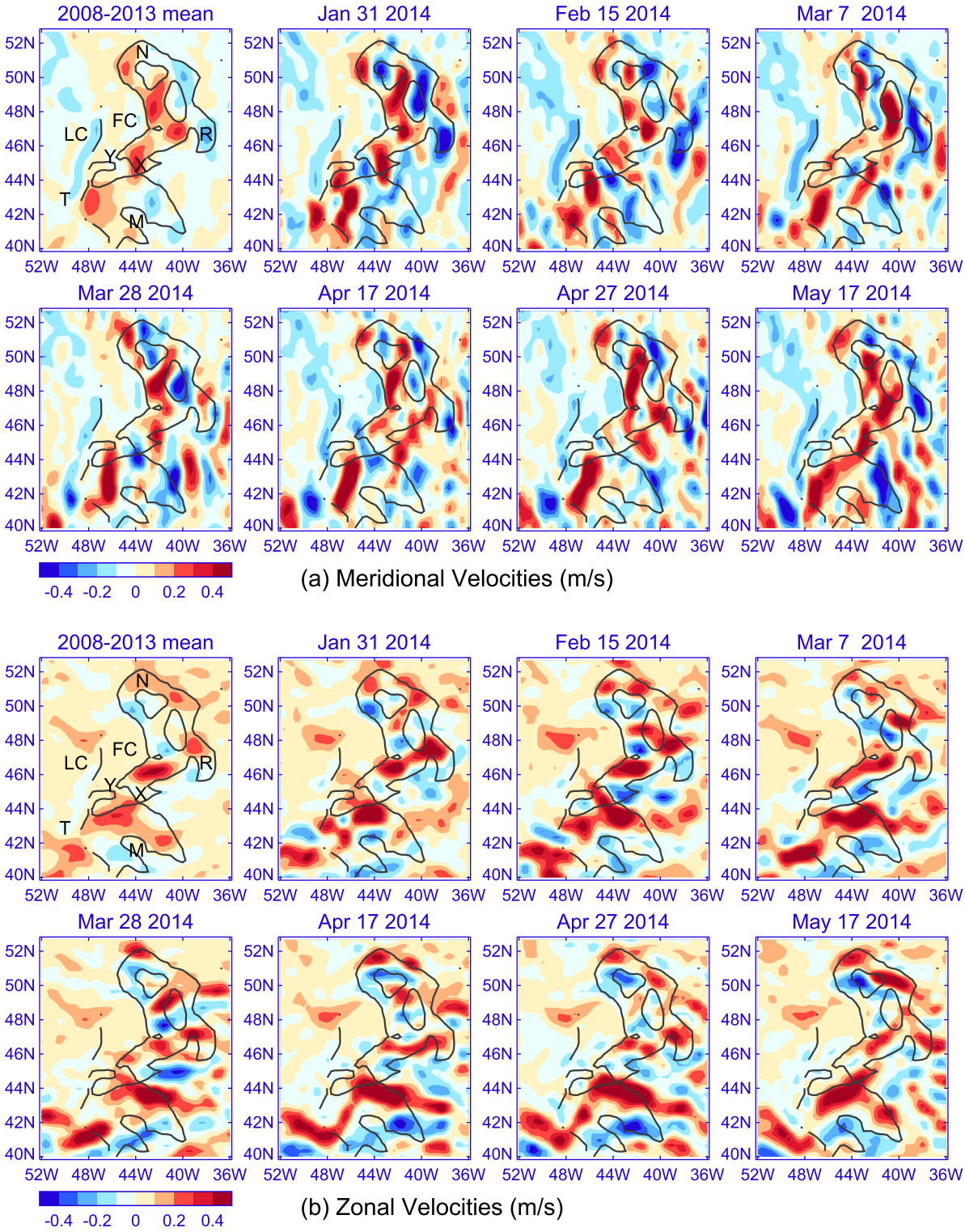

Fig. 8 **(a)** Meridional and (**b**) zonal components of surface current velocity in the Newfoundland Basin in January–May 2014. The first panel in each dataset represents the pattern for the 5y (2008-2013) mean values of current velocity. LC is Labrador Current, M is Mann Eddy, N is Northwest Corner, R is the Newfoundland Basin Return Current, T is the TGB, FC is the Flemish Cap and X and Y mark alternative exit points of the NAC from the Mann Eddy. The black outline represents the path of the NAC derived from Figure 1b. Color bar denotes velocities in m/s.

To confirm the apparent surface current direction reversal illustrated in Fig. 8 and to place it in a longer- term perspective, we examined the time series of meridional surface current velocity at 44.5–45°N 44–43.5°W, just north of the main exit from the Mann Eddy (X in Fig. 8) and virtually coincident with the CFP (Fig. 4). Fig. 9a shows the monthly

2026 La Société canadienne de météorologie et d'océanographie

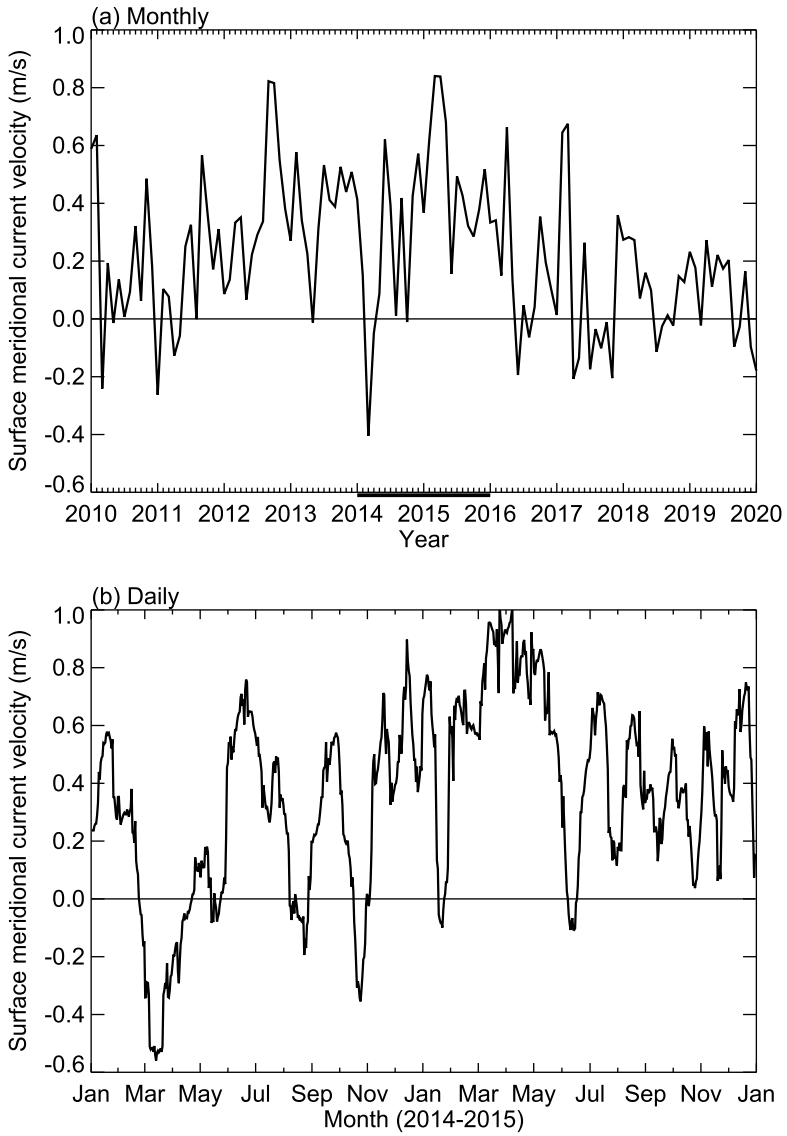

Fig. 9 Time series of meridional surface current velocity (m/s) at 44.5°–45 °N 44 °–43.5 °W between (a) 2010 and 2020 (monthly data) and (b) in 2014 and 2015 (daily data) where northward motion is positive. The range between 2014 and 2016 identified by the horizontal bar on the x axis in (a) is shown expanded in (b).

time series from 2010–2020 and as expected, confirms that for most of this period, flow was northwards (positive). However, between February and March 2014 there was a large surface current reversal in the path of the NAC from about 0.4 m/s northwards to about 0.5 m/s southwards, a change unmatched over a period of 20y. Fig. 9b represents the daily data between 2014 and 2015 and shows that the trough of current velocity is on March 12th 2014 and reaches 0.6 m/s southwards compared with a value of about 0.6 m/s northwards immediately before and after the 2014 event. This dramatic redirection of the NAC surface waters is consistent with the insertion of a strong south-flowing current into path of the NAC as implied by Fig. 8a (February 15 to April 17). Similar but smaller events were dated as August 22 and October 23 2014 and January 21 and June 15 2015. It is notable that these current- reversal events approximately coincided with the cooling and freshening events identified in the time series of heat and salt anomalies seen in Fig. 3c,d (March, September-November 2014 and June-July 2015).

4 Discussion

In contrast to the widely-mooted possibility that a reduction of heat input from the Gulf Stream into the NAC might lead to a cooling of the SPNA, this work provides evidence that the unprecedented 2014–2016 cooling and freshening of the SPNA (the cold fresh anomaly or CFA) was the consequence of a temporary hiatus in transport of warm salty water in the NAC soon after it separated from the Mann Eddy near 44.5°N 43.5°W (X in Fig. 1). Thus, for early 2014 we are not

2026 Canadian Meteorological and Oceanographic Society

proposing a reduction of transmission of heat and salt in the GS but rather a transport hiatus in the proximal NAC which would have similar effects in cooling and freshening the SPNA. The consequence of such a transport interruption in the NAC is that heat and salt not reaching the distal NAC would have to go elsewhere and here we suggest that much of this diverted heat and salt returns westwards via known recirculation pathways (R1, R2 Fig. 1a) and explains the increased heat and salt near the North American seaboard (WSA) which forms heat and salt dipoles with the CFA in 2014–2016. We cannot exclude the possibility that a slowing or cessation of northeasterly transmission of heat and salt in the NAC might also slow the rate of transport in the GS leading to an accumulation of warm salty water in the subtropical North Atlantic.

In this work we largely concentrate on the initial events in early 2014 although similar but subsidiary events seem to have occurred in late 2014 and early 2015 (Fig. 3 and Fig. 9b). These would have augmented the initial changes seen in February/March 2014 and can partly explain why only about a quarter of the heat and salt changes of July 2015 can be seen in March 2014 (Fig. 4). This is a dynamic situation where it is difficult to accurately account not only for the effects of the length and strength of the original stimulus but also for the manifold ways in which heat and salt changes were delocalized subsequently (see section 2). These large and rapid changes in the distribution of heat and salt across the North Atlantic in 2014–2016 may have presaged the cold summer in Northern Europe and warm summer in Southern Europe in 2015 (Duchez et al., 2016; Herring et al., 2016; Oltmanns et al., 2024; Yin et al., 2018).

In the period 2014–2016, approximately equivalent amounts of heat and salt were lost from the CFA region in the SPNA as were gained by the region along the path of the GS close to the North American coast (Fig. 2,3,6). Such observations recall the findings of Grist et al. (2016), Robson et al. (2016) and Frajka-Williams et al., 2017) with regard to temperature anomalies, Holliday et al. (2020) who considered salinity data since 1950, and especially Bryden et al. (2020) who showed an approximately inverse relationship between the reductions of salt and heat centred on 48°N 30°W (equivalent to our CFA) and rises in these parameters near the North American coastal region (our WSA) in 2014–16. They considered the possibility that the cooling of the SPNA since 2008 was due to a decrease in delivery of warm saline water from the subtropics and that this mechanism might also explain why there was warming in the region north of 26°N. However, it was difficult to point to any alteration in the magnitude of heat and salt transport in the GS measured at 26°N-40°N which could explain the 2014–2016 events (see Introduction). Our present results support this idea that the heat and salt dipoles observed in 2015 (Fig. 2) are indicators of prior interruption/diversion of heat and salt delivery but we provide evidence that the most significant lesion is in in the proximal NAC as it exits the Mann Eddy and not in the GS.

One of the pillars of our concept of the evolution of the CFA in 2014–16 is the realization that the fine structure of the CFA represents the reticulations of the NAC as it crosses the MAR i.e. the CFA is not an amorphous 'cold blob' (Desbruyères et al., 2019; Frajka-Williams et al., 2017; Josey et al., 2018) but a manifestation of the intricate normal path of the NAC as it is forced to branch and slow while negotiating the geomorphological complexities of the MAR (Fig. 6,7). This possibility was implied from the results of Stendardo et al. (2020) for salinity (their Fig. 5) but it has not previously been confirmed with SST and SSH data (Fig. 6,7).

An important feature of the development of the CFA is that the dipoles of salt and heat anomalies visible in 2015 (Fig. 2) first appeared in early 2014 (Fig. 5, Fig. 6) as the CFP. These initial dipoles were seen in a relatively small area with the positive poles (WSP) centered near 41°N 51°W and the negative poles (CFP) at 44°N 42°W, almost two thousand kilometres from the positions of the WSA and CFA in 2015 (Fig. 2). However, the CFP and WSP accounted for at least a quarter of the heat and salt anomalies of those in the CFA and WSA more than a year later (Fig. 4b,c). The CFP appeared initially at 45°N 42°W close to the exit of the NAC from the Mann Eddy (X in Fig. 1b) and appeared to evolve along the path of the NAC (Fig. 5,6) where it eventually spread through the reticulations of the MAR and manifested as the CFA (Fig. 2). Studies of surface current velocity in February/March 2014 (Fig. 8,9) identified a reversal of the current direction in the normal path of the NAC close to where the NAC emerges from the Mann Eddy at 44°N 43°W. The position and time development of this feature was almost identical to that of the CFP, so we are led to propose that the CFP at 45°N 42°W and the surface current reversal at 44°N 43°W are different aspects of a singular lesion in the proximal NAC which reduced the amount of heat and salt transmitted downstream to the distal NAC and eventually the CFA. Thus, there could be only an indirect relationship between the CFP and CFA: the CFP is the site of a block in NAC transmission caused by a cold fresh current and the CFA is the path of the NAC cooled and freshened as a consequence of that block.

Significantly, the time series of the episodes of current reversal in the NAC beginning in February–March 2014 (Fig 9b) appears to resemble the time series of cooling and freshening of the CFA (Fig. 3c,d) suggesting a direct relationship between blocking of the normal northward progress of the NAC at X and cooling and freshening of the SPNA.

We emphasise that the maximum salt deficit in the CFA in July 2015, equivalent to about 10,000km^3 of fresh water agrees fairly well with the estimate obtained by Holliday et al. (2020) (about 7000km^3). This is a prodigious amount, an order of magnitude larger than the 1000km^3 per year of freshwater equivalent for each of the Great Salinity Anomalies of the late 20th century (Allan & Allan, 2024; Belkin et al., 1998) and more than the total loss of water from Greenland ice melt in the last 20 years (https://

2026 La Société canadienne de météorologie et d'océanographie

polarportal.dk/en/greenland/mass-and-height-change/). Not only is the 2014 event large but it is also rapid, with at least a quarter of the change occurring within a month or two. We visualize that this is the magnitude of the flow of local cold fresher water required to replace the warm saltier water 'missing' from the NAC in 2014 due to the initial flow hiatus in the NAC close to its point of separation from the Mann Eddy near 44°N 43°W (Fig. 8b).

The formation of the CFP most likely happened because an initial deficit of warm salty water in the NAC at X precipitated an inflow of cold fresh local water which was faster than the rate at which it could be dissipated by transmission along the NAC. Current flow in the NAC was > 50cm/s in the rising limb of the Mann Eddy and to the east of Flemish Cap but at the exit from the Mann Eddy where the CFP accumulated in early 2014 (X in Fig. 1b) it was 10–20cm/s (Fratantoni, 2001; Reverdin et al., 2003) so could represent a pinch point in NAC flow where the NAC passed through a narrow gap between seamount groups (Fig. 1b). The subsequent accumulation of heat and salt deficit in the CFA can be attributed to the slowing and spreading of the NAC as it passed through the fenestrations of the MAR.

Although we favour the NAC flow hiatus explanation for the development of the CFA, we recognize the possibility mooted most specifically by Holliday et al. (2020) that the cooling and freshening of the eastern SPNA is due to enhanced (probably wind-driven) input of cold fresh water from the LC. We take this proposition very seriously particularly because there is evidence from Fig. 8a for apparent incursions of LC/DWBC water into the NAC near its exit (X) from the Mann Eddy and into the Mann Eddy itself in February -March 2014 (Fig. 8b). It is plausible that the influx of cold fresh water from the LC/DWBC is itself the direct source of the cooling and freshening of the CFA. In that case however, it is not easy to explain the magnitude and the rapidity of the changes in heat and salt observed in the CFP and WSP or even the existence of the positive arm of the trans-Atlantic dipole (WSA) (Fig. 4,5) from the enhanced LC input envisaged by Holliday et al. (2020). Thus, even if 10% (1 Sv) of the entire flow of the LC (about 10Sv; Jutras et al., 2023) entered the NAC in a month in 2014, this would be <1% of the flow of the NAC (> 100Sv; Mertens et al., 2014). The mean salinity of the LC (0–400m) is about 34.5psu (Ma et al., 2022) while the salinity of the NAC is about 35.5 (Fig. 5) so there seems little likelihood that the observed reduction in salinity of the NAC in March 2014 (0.4psu, Fig. 5) could be achieved simply by mixing in such a relatively small amount of LC water. Likewise, the influx of the fresh water represented by such a quantity of LC flow (about 3% of 1 Sv or <100 km^3 in a month) would be dwarfed by the observed 10,000 km^3 accumulation of fresh water in the CFA in 2014. Finally, we found no evidence for strong eastward-directed winds over the LC in early 2014 or a significant weakening of the main LC southward flow which is essentially a near-surface current and is less likely to influence the deep regions of the NAC.

A more likely candidate than the LC for a cold fresh current which could cool and freshen the NAC and create the CFA would be the DWBC (Fig. 1b). This not only has the flow capacity (30 Sv) to affect the NAC but is deep enough and close enough to interact with the full depth of the NAC from north of the Flemish Cap to the Tail of the Grand Banks (Mertens et al., 2014; Zantopp et al., 2017). Bearing in mind that Labrador Sea Water (LSW) appears to constitute the top 1000m of the DWBC (Zantopp et al., 2017) we need to think in terms of the interaction of NAC with LSW rather than with the whole depth of the DWBC. It is plausible that an influx of LSW from the DWBC could cool and freshen the NAC resulting in the formation of the CFA in 2014–2015. However, it is difficult to see how such a cold fresh input could be linked to warming and salinifying the WSP and WSA unless collision with the DWBC (LSW) interrupted transport in the NAC.

There have been previous strong suggestions that the cooling of the eastern SPNA (CFP) might be initiated and sustained by cold winds from the northwest, particularly in the severe North American winter of 2014 (Grist et al., 2016; Josey et al., 2018; Sanders et al., 2022). We think this is unlikely to be a determining factor because (a) plausible surface atmosphere-ocean exchanges would not have the capacity or lateral spread to explain the magnitude of the drop in ocean heat content extending down to 700m over millions of square km in early 2014 (monthly anomalies in air–sea heat fluxes computed from an atmospheric reanalysis were an order of magnitude too small to explain the observed cooling down to 400m); (b) atmospheric drivers could not easily have given rise to the parallel drop in salinity in the CFA; (c) the CFP which appears to represent the first manifestation of the heat/salinity dipole is too far south and west to be reached by sub-arctic winds. We would not exclude the possibility that strong subarctic winds might displace cold currents eastwards towards the NAC as partly suggested by Holliday et al. (2020). Additionally, it is plausible that atmospheric responses to the substantial ocean surface anomalies and subsequent air–sea heat exchanges subsequently contributed to the evolution and persistence of the cold, fresh region (e.g. Josey et al., 2018).

Thus, it appears that only a hiatus in NAC flow could explain such large changes in heat and salinity in the Newfoundland Basin and their development into the heat and salinity dipoles (WSP and CFP) which subsequently give rise to the WSA and CFA (Fig. 4,5). We are open to the possibility that the initiation of the hiatus might have involved an unusual influx of LC/DWBC water from the west through the Y gap into the NAC near its exit (X) from the Mann Eddy because this is supported by our evidence (Fig. 8a,b) and would be consistent with the enhanced inflow of cold fresh water from the west (the LC) which was identified by Holliday et al. (2020). However, we are suggesting that the major cooling and freshening influence on the NAC in 2014 was

2026 Canadian Meteorological and Oceanographic Society

not from the west but from the east (Fig. 8b), probably to replace warmer, saltier waters no longer reaching the NAC north of X.

Of course, the current velocity data only relates directly to surface currents which may not be a good guide to what is happening at depth and we leave open the possibility that deep cold currents associated with the DWBC have the potential to deflect the path of the NAC, not only near the northern exit of the Mann Eddy (X) but also by deflecting eastward the western limb of the Mann Eddy (Fig. 8) in early 2014. This work has largely concerned the evolution of the CFA and we are aware that at present we have no comparable mechanism for the evolution of the positive arm of the dipole which is first seen as the WSP close to the tip of the Grand Banks (Fig. 4, Fig. 5).

At present it is difficult to explain why a transport hiatus in the NAC should have occurred in 2014–2015 but not apparently before or after (Fig. 3, Fig. 9a). However, if a sudden cooling and freshening of the SPNA is taken as an indication of a NAC transport hiatus, there are many years when there was a slight cooling and freshening in the SPNA in early spring (Fig. 3) but it was only in 2014–15 that this was sustained and intensified. Future such events should be recognizable by the appearance of sudden dipolar anomalies of heat and salt in the path of the NAC which evolve into a cooling/freshening of the SPNA and warming/salinification of the North American seaboard. There might also be indications of current reversal near the northern exit (X) of the NAC from the Mann Eddy (Fig. 9a,b). We continue to explore the particular circumstances which made 2014 so unusual in the hope of finding the mechanism of the putative interruption of the NAC. We want to pinpoint the initial changes in the NAC and to examine the possible effects of a transport hiatus in the NAC on the pattern of transport in the GS.

There has been much speculation in the scientific literature and even in popular news media regarding the possibility and climate consequences of a reduced flow in the GS promoted by increasing global temperatures. Rather than a change in GS output, we have identified an interruption of NAC flow in early 2014 near 44°N 43°W and this is likely to have had effects similar to a reduction in GS flow. The NAC at this point forms part of the **rising** limb of AMOC so an interruption of flow in the NAC would reduce AMOC, with potential consequences for the climate of the North Atlantic region (Rahmstorf, 2024) and perhaps for global circulation. Such effects would be compounded if invasion of the proximal NAC by DWBC water is part of the mechanism by which the transport hiatus occurs (Fig. 8) because the DWBC is a component of the **descending** limb of AMOC. Measuring variations in AMOC strength directly are problematic but if we are now able to associate weakening of transport in the NAC with formation of the trans-Atlantic heat and salt dipoles and reversal of current direction at the exit from the Mann Eddy (X), these may represent new and simpler observational methods of flagging up possible reductions in AMOC strength.

Acknowledgements

The authors are grateful to Robert Marsh, an anonymous reviewer and the editors for their constructive input on the manuscript.

Disclosure statement

No potential conflict of interest was reported by the author(s).

Funding

Richard Allan received support from the Research Councils UK (RCUK) National Centre for Earth Observation (grant numbers NE/RO16518/1 and NE/Y006216/1).

Data availability statement

The input data and methods used in this analysis originate from publicly available sources as detailed in Section 2.

ORCID

David Allan http://orcid.org/0000-0002-2069-0315
Richard P. Allan https://orcid.org/0000-0003-0264-9447

References

Allan, D., & Allan, R. P. (2019). Seasonal changes in the North Atlantic cold anomaly: The influence of cold surface waters from coastal Greenland and warming trends associated with variations in subarctic sea ice cover. *Journal of Geophysical Research: Oceans*, *124*, 9040–9052. https://doi.org/10.1029/2019JC015379

Allan, D., & Allan, R. P. (2024). Odden ice melt linked to Labrador Sea ice expansions and the great salinity anomalies of 1970-1995. *Journal of Geophysical Research: Oceans*, *129*, e2023JC019988. https://doi.org/10.1029/2023JC019988

Allan, D., & Allan, R. P. (2025). Influence of meltwater from Labrador Sea ice and icebergs transported via the Flemish Cap on the long-term North Atlantic cold anomaly. *Atmosphere-Ocean*, *63*(1), 21–38. https://doi.org/10.1080/07055900.2025.2478832

Belkin, I. M., Levitus, S., Antanov, J., & Malmberg, S.-A. (1998). "Great salinity anomalies" in the North Atlantic. *Progress in Oceanography*, *41*(1), 1–68. https://doi.org/10.1016/S0079-6611(98)00015-9

Boers, N. (2021). Observation-based early-warning signals for a collapse of the Atlantic meridional overturning circulation. *Nature Climatic Change*, *11*, 680–688. https://doi.org/10.10.38/s41558-021-01097-4

Bower, A. S., & von Appen, W.-J. (2008). Interannual variability in the pathways of the North Atlantic current over the Mid-Atlantic ridge and the impact of topography. *Journal of Physical Oceanography*, *38*, 104–120. https://doi.org/10.1175/2007JPO3686.1

Breckenfelder, T., Rhein, M., Roessler, A., Böning, C. W., Biastoch, A., Behrens, E., & Mertens, C. (2017). Flow paths and variability of the North Atlantic current: A comparison of observations and a high-resolution

2026 La Société canadienne de météorologie et d'océanographie

model. *Journal of Geophysical Research: Oceans*, *122*, 2686–2708. https://doi.org/10.1002/2016JC012444

Bryden, H. L., Johns, W. E., King, B. A., McCarthy, G., McDonagh, E. L., Moat, B. I., & Smeed, D. A. (2020). Reduction in ocean heat transport at 26°N since 2008 cools the eastern subpolar gyre of the North Atlantic Ocean. *Journal of Climate*, *33*, 1677–1689. https://doi.org/10.1175/JCLI-D-19-0323.1

Bubnov, V. S. (1995). The North Atlantic current by the Atlantex90 experiment data. *Oceanology*, *34*, 733–737.

Caesar, L., McCarthy, G. D., Thornalley, G. J. R., Cahill, N., & Rahmstorf, S. (2021). Current Atlantic meridional overturning circulation weakest in last millennium. *Nature Geoscience*, *14*, 118–120. https://doi.org/10.1038/s41561-021-00699-z

Caesar, L., Rahmstorf, S., Robinson, A. Feulner, G. Saba, V. (2018). Observed fingerprint of a weakening Atlantic Ocean overturning circulation. *Nature*, *556*, 191–196. https://doi.org/10.1038/s41586-018-0006-5

Caldeira, M. A., & Reis, J. C. (2017). The azores confluence zone. *Frontiers in Marine Science*, *4*), https://doi 10.3389fmars.2017.00037

Carr, M.-E., & Rossby, H. T. (2001). Pathways of the North Atlantic current from surface drifters and subsurface floats. *Journal of Geophysical Research: Oceans*, *106*(C3), 4405–4419. https://doi.org/10.1029/2000JC900106

Daniault, N., Mercier, H., Lherminier, P., Sarafanov, A., Falina, A., Zunino, P., Pérez, F. F., Ríos, A. F., Ferron, B., Huck, T., Thierry, V., & Gladyshev, S. (2016). The northern North Atlantic Ocean mean circulation in the early 21st century. *Progress in Oceanography*, *146*, 142–158. https://doi.org/10.1016/j.pocean.2016.06.007.

Desbruyères, D. G., Mercier, H., Maze, G., & Daniault, N. (2019). Surface predictor of overturning circulation and heat content change in the subpolar North Atlantic. *Ocean Science*, *15*, 809–817. https://doi.org/10.5194/os-15-809-2019

Dima, M., & Lohmann, G. (2010). Evidence for two distinct modes of large-scale ocean circulation changes over the last century. *Journal of Climate*, *23*(1), 5–16. https://doi.org/10.1175/2009JCLI2867.1

Dong, S., Baringer, M. O., & Goni, G. J. (2019). Slowdown of the Gulf Stream during 1993-2016. *Scientific Reports*, *9*(1), 6672. https://doi.org/10.1038/s41598-019-42820-8

Drijfhout, S., van Oldenborgh, G. J., & Cimatoribus, A. (2012). Is a decline of AMOC causing the warming hole above the North Atlantic in observed and modelled warming patterns? *Journal of Climate*, *25*, 8373–8379. https://doi.org/10.1175/JCLI-D-12-00490.1

Duchez, A., Frajka-Williams, E., Josey, S. A., Evans, D. G., Grist, J. P., Marsh, R., McCarthy, G. D., Sinha, B., Berry, D. I., & Hirschi, J. J.-M. (2016). Drivers of exceptionally cold North Atlantic Ocean temperatures and their link to the 2015 European heat wave. *Environmental Research Letters*, *11*(7), https://doi.org/10.1088/1748-9326/11/7/074004

Frajka-Williams, E., Beaulieu, C., & Duchez, A. (2017). Emerging negative Atlantic multidecadal oscillation index in spite of warm subtropics. *Scientific Reports*, *7*, 11224. https://doi.org/10.1038/s41598-017-11046-x

Fratantoni, D. M. (2001). North Atlantic surface circulation during the 1990′s observed with satellite-tracked drifters. *Journal of Geophysical Research: Oceans*, *106*(C10), 22067–22093. https://doi.org/10.1029/2000JC000730

Fratantoni, P. S., & McCartney, M. S. (2010). Freshwater export from the LC to the North Atlantic current at the tail of the grand banks of Newfoundland. *Deep Sea Research Part I: Oceanographic Research Papers*, *57*(2), 258–283. https://doi.org/10.1016/j.dsr.2009.11.006

Gervais, M., Shaman, J., & Kushnir, Y. (2018). Mechanisms governing the development of the North Atlantic warming hole in the CESM-LE future climate simulations. *Journal of Climate*, *31*, 5927–5946. https://doi.org/10.1175/JCLI-D-17-0635.1

Gonçalves Neto, A., Langan, J. A., & Palter, J. B. (2021). Changes in the Gulf Stream preceded rapid warming of the northwest Atlantic shelf. *Communications Earth & Environment*, *2*(74), https://doi.org/10.1038/s43247-021-00143-5

Good, S. A., Martin, M. J., & Rayner, N. A. (2013). EN4: quality-controlled ocean temperature and salinity profiles and monthly objective analyses with uncertainty estimates. *Journal of Geophysical Research: Oceans*, *118*, 6704–6716. https://doi.org/10.1002/2013JC009067

Gouretski, V. and Reseghetti, F. (2010). On depth and temperature biases in bathythermograph data: Development of a new correction scheme based on analysis of a global ocean database. *Deep Sea Research Part I: Oceanographic Research Papers*, *57*(6), 812–833. https://doi.org/10.1016/j.dsr.2010.03.011

Grist, J. P., Josey, S. A., Jacobs, Z. L., Marsh, R., Sinha, B., & Van Sebille, E. (2016). Extreme air–sea interaction over the North Atlantic subpolar gyre during the winter of 2013–2014 and its sub-surface legacy. *Climate Dynamics*, *46*(11), 4027–4045. https://doi.org/10.1007/s00382-015-2819-3

Han, G., Lu, Z., Wang, Z., Helbig, J., Chen, N., & de Young, B. (2008). Seasonal variability of the LC and shelf circulation off Newfoundland. *Journal of Geophysical Research: Oceans*, *113*, C10013. https://doi.org/10.1029/2007JC004376

Herring, S. C., A. Hoell, M. P. Hoerling, J. P. Kossin, C. J. Schreck III, and P. A. Stott. (2016). Explaining extreme events of 2015 from a climate perspective. *Bulletin of the American Meteorological Society*, *97* (12), S1–S145. https://doi.org/10.1175/BAMS-ExplainingExtremeEvents2015.1

Hersbach, H., Bell, B., Berrisford, P., Hirahara, S., Horányi, A., Muñoz-Sabater, J., Muñoz-Sabater, J., Nicolas, J., Peubey, C., Radu, R., Schepers, D., Simmons, A., Abdalla, S., Abellan, X., Balsamo, G., Bechtold, P., Biavati, G., Bidlot, J., Bonavita, M., … Thépaut, J. (2020). The ERA5 global reanalysis. *Quarterly Journal of the Royal Meteorological Society*, *146*(730), 1999–2049. https://doi.org/10.1002/qj.3803.

Holliday, N. P., Bersch, M., Berx, B., Chafik, L., Cunningham, S., Florindo-López, C., Hátún, H., Johns, W., Josey, S. A., Larsen, K. M. H., Mulet, S., Oltmanns, M., Reverdin, G., Rossby, T., Thierry, V., Valdimarsson, H., & Yashayaev, I. (2020). Ocean circulation causes the largest freshening event for 120 years in eastern subpolar North Atlantic. *Nature Communications*, *11*, 585. https://doi.org/10.1038/s41467-020-14474-y.

Jacobs, Z. L., Grist, J. P., Marsh, R., Sinha, B., & Josey, S. A. (2020). The major role of air-sea heat fluxes in driving interannual variations of Gulf Stream transport. *Journal of Geophysical Research: Oceans*, *125*, e2019JC016004. https://doi.org/10.1029/2019JC016004.

Josey, S. A., Hirschi, J. J.-M., Sinha, B., Duchez, A., Grist, J. P., & Marsh, R. (2018). The recent Atlantic cold anomaly: Causes, consequences and related phenomena. *Annual Review of Marine Science*, *10*(1), 475–501. https://doi.org/10.1146/annurev-marine-121916-063102

Jutras, M., Dufour, C. O., Mucci, A., & Talbot, L. C. (2023). Large-scale control of the retroflection of the Labrador Current. *Nature Communications*, *14*, 2623. https://doi.org/10.1038/s41467-023-38321-y

Keil, P., Mauritsen, T., Jungclaus, J., Hedemann, C., Olonscheck, D. & Ghosh, R. (2020). Multiple drivers of the North Atlantic warming hole. *Nature Climate Change*, *10*, 667–671. https://doi.org/10.1038/s41558-020-0819-8

Kelly, K. A., Singh, S., & Huang, R. X. (1998). Seasonal variations of sea surface height in the Gulf Stream region. *Journal of Physical Oceanography*, *29*, 313–327. https://doi.org/10.1175/1520-0485(1999)029<0313:SVOSSH>2.0.CO;2

Klein, B., & Siedler, G. (1989). On the origin of the azores current. *Journal of Geophysical Research: Oceans*, *94*, 6159–6168. https://doi.org/10.1029/JC094iC05p06159

Krauss, W., Käse, R. H., & Hinrichsen, H.-H. (1990). The branching of the Gulf Stream southeast of the grand banks. *Journal of Geophysical Research: Oceans*, *95*(C8), 13089–13103. https://doi.org/10.1029/JC095iC08p13089

Lazier, J. R. N. (1994). Observations in the northwest corner of the North Atlantic current. *Journal of Physical Oceanography*, *24*(7), 1449–1463

Li, L., Lozier, M. S., & Li, F. (2022). Century-long cooling trend in subpolar North Atlantic forced by atmosphere: An alternative explanation. *Climate Dynamics*, *58*, 2249–2267. https://doi.org/10.1007/s00382-021-06003-4

Liu, C., Allan, R. P., Mayer, M., Hyder, P., Desbruyeres, D., Cheng L., Xu, J., Xu F., & Zhang, Y. (2020). Variability in the global energy budget and transports 1985–2017. *Climatic Dynamics*, *55*, 3381–3396. https://doi.org/10.1007/s00382-020-05451-.8.

2026 Canadian Meteorological and Oceanographic Society

Ma, Y., Lu, Y., Hu, X., Gilbert, D., Scott, A., Socolofsky, S. A., & Boufadel, M. (2022). Model simulated freshwater transport along the Labrador Current east of the grand banks of Newfoundland. *Frontiers in Marine Science*, *9* (Physical Oceanography). https://doi.org/10.3389/fmars.2022.908306.

Mann, C. R. (1967). The termination of the gulf stream and the beginning of the North Atlantic current. *Deep Sea Research and Oceanographic Abstracts*, *14*, 337–359. https://doi.org/10.1016/0011-7471(67)90077-0

Mertens, C., Rhein, M., Walter, M., Böning, C. W., Behrens, E., Kieke, D., Steinfeldt, R., & Stöber, U. (2014). Circulation and transports in the Newfoundland Basin, western subpolar North Atlantic. *Journal of Geophysical Research: Oceans*, *119*, 7772–7793. https://doi.org/10.1002/2014JC010019

Oltmanns, M., Holliday, N. P., Screen, J., Moat, B. I., Josey, S. A., Evans, D. G., & Bacon, S. (2024). European summer weather linked to North Atlantic freshwater anomalies in preceding years. *Weather and Climate Dynamics*, *5*, 109–132. https://doi.org/10.5194/wcd-5-109-2024

Palter, J. B. (2015). The role of the Gulf Stream in European climate. *Annual Review of Marine Science*, *7*(1), 113–137. https://doi.org/10.1146/annurev-marine-010814-015656

Pardaens, A. K., Gregory, J. M., & Lowe, J. A. (2011). A model study of factors influencing projected changes in regional sea level over the twenty-first century. *Climate Dynamics*, *36*, 2015–2033. https://doi.org/10.1007/s00382-009-0738-x

Pérez-Brunius, P., Rossby, T., & Watts, D. R. (2004). Absolute transports of mass and temperature for the North Atlantic current– subpolar front system. *Journal of Physical Oceanography*, *34*, 1870–1883.

Qiu, B. (1994). Determining the mean gulf stream and its recirculations through combining hydrographic and altimetric data. *Journal of Geophysical Research: Oceans*, *99*(C1), 951–962. https://doi.org/10.1029/93JC03033

Rahmstorf, S. (2024). Is the Atlantic overturning circulation approaching a tipping point? *Oceanography*, https://doi.org/10.5670/oceanog.2024.501

Rahmstorf, S., Box, J., Feulner, G., Mann, M., Robinson, A., Rutherford, S., & Schaffernicht, E. (2015). Exceptional twentieth-century slowdown in Atlantic Ocean overturning circulation. *Nature Climate Change*, *5*, 475–480. https://doi.org/10.1038/nclimate2554.

Reverdin, G., Niiler, P. P., & Valdimarsson, H. (2003). North Atlantic Ocean surface currents. *Journal of Geophysical Research: Oceans*, *108*(C1), 3002. https://doi.org/10.1029/2001JC001020

Robson, J., Ortega, P., & Sutton, R. (2016). A reversal of climatic trends in the North Atlantic since 2005. *Nature Geoscience*, *9*, 513–517. https://doi.org/10.1038/ngeo2727

Roquet, F., Ferreira, D., Caneill, R., Schlesinger, D., & Madec, G. (2022). Unique thermal expansion properties of water key to the formation of sea ice on earth. *Science Advances*, *8*, 46. https://doi.org/10.1126/sciadv.abq0793

Rossby, T. (1996). The North Atlantic current and surrounding waters: At the crossroads. *Reviews of Geophysics*, *34*(4), 463–481. https://doi.org/10.1029/96RG02214

Sanders, R. N. C., Jones, D. C., Josey, S. A., Sinha, B., & Forget, G. (2022). Causes of the 2015 North Atlantic cold anomaly in a global state estimate. *Ocean Science*, *18*(4), 953–978. https://doi.org/10.5194/os-18-953-2022

Seidov, D., Mishonov, A., Reagan, J., & Parsons, R. (2019). Resilience of the Gulf Stream path on decadal and longer timescales. *Scientific Reports*, *9*, 11549. https://doi.org/10.1038/s41598-019-48011-9

Solodoch, A., McWilliams, J. C., Stewart, A. L., Gula, J., & Renault, L. (2020). Why does the deep western boundary current "leak" around Flemish Cap? *Journal of Physical Oceanography*, *50*, 1989–2016. https://doi.org/10.1175/JPO-D-19-0247.1

Stendardo, I., Rhein, M., & Hollmann, R. (2016). A high resolution salinity time series 1993–2012 in the North Atlantic from argo and altimeter data. *Journal of Geophysical Research: Oceans*, *121*, 2523–2551. https://doi.org/10.1002/2015JC011439

Stendardo, I., Rhein, M., & Steinfeldt, R. (2020). The North Atlantic current and its volume and freshwater transports in the subpolar North Atlantic, time period 1993–2016. Journal of Geophysical Research: Oceans, 125, e2020JC016065. https://doi.org/10.1029/2020JC016065.

Yin, J., Overpeck, J., Peyser, C., & Stouffer, R. (2018). Big jump of record warm global mean surface temperature in 2014–2016 related to unusually large oceanic heat releases. *Geophysical Research Letters*, *45*, 1069–1078. https://doi.org/10.1002/2017GL076500

Zantopp, R., Fischer, J., Visbeck, M., & Karstensen, J. (2017). From interannual to decadal: 17 years of boundary current transports at the exit of the Labrador Sea. *Journal of Geophysical Research Oceans*, *122*, 1724–1748. https://doi:10.10022016JC012271

2026 La Société canadienne de météorologie et d'océanographie